Thriving or surviving? The isotopic record of the Wrangel Island woolly mammoth population

Arppe, Laura

2019-10-15

Arppe , L , Karhu , J A , Vartanyan , S , Drucker , D G , Etu-Sihvola , H & Bocherens , H 2019 , ' Thriving or surviving? The isotopic record of the Wrangel Island woolly mammoth population ' , Quaternary Science Reviews , vol. 222 , 105884 . https://doi.org/10.1016/j.quascirev.2019.105884

http://hdl.handle.net/10138/309133
https://doi.org/10.1016/j.quascirev.2019.105884

Quaternary Science Reviews 222 (2019) 105884

Contents lists available at ScienceDirect

Quaternary Science Reviews

journal homepage: www.elsevier.com/locate/quascirev

Thriving or surviving? The isotopic record of the Wrangel Island woolly mammoth population

Laura Arppe [a, *], Juha A. Karhu [b], Sergey Vartanyan [c], Dorothée G. Drucker [d], Heli Etu-Sihvola [a], Hervé Bocherens [d, e]

[a] Finnish Museum of Natural History LUOMUS, P.O. Box 64 00014, University of Helsinki, Helsinki, Finland
[b] Department of Geosciences and Geography, P.O.Box 64 00014, University of Helsinki, Helsinki, Finland
[c] North-East Interdisciplinary Scientific Research Institute n.a. N.A. Shilo, Far East Branch, Russian Academy of Sciences (NEISRI FEB RAS), 16 Portovaya Str., 685000 Magadan, Russia
[d] Senckenberg Centre for Human Evolution and Palaeoenvironment (S-HEP), Sigwartstr. 10, 72076 Tübingen, Germany
[e] Department of Geosciences, Biogeology, University of Tübingen, Hölderlinstr. 12, 72074 Tübingen, Germany

ARTICLE INFO

Article history:
Received 28 February 2019
Received in revised form
27 June 2019
Accepted 13 August 2019
Available online xxx

Keywords:
Holocene
Pleistocene
Paleoclimatology
Paleoecology
Russia
Beringia
Stable isotopes
Radiogenic isotopes
Mammoths
Extinction

ABSTRACT

The world's last population of woolly mammoths (*Mammuthus primigenius*) lived on Wrangel Island persisting well into the Holocene, going extinct at ca. 4000 cal BP. According to the frequency of radiocarbon dated mammoth remains from the island, the extinction appears fairly abrupt. This study investigates the ecology of the Wrangel Island mammoth population by means of carbon, nitrogen and sulfur isotope analyses. We report new isotope data on 77 radiocarbon dated mammoth specimens from Wrangel Island and Siberia, and evaluate them in relation to previously published isotope data for Pleistocene mammoths from Beringia and lower latitude Eurasia, and the other insular Holocene mammoth population from St. Paul Island. Contrary to prior suggestions of gradual habitat deterioration, the nitrogen isotope values of the Wrangel Island mammoths do not support a decline in forage quality/quantity, and are in fact very similar to their north Beringian forebears right to the end. However, compared to Siberian mammoths, those from Wrangel Island show a difference in their energy economy as judged by the carbon isotope values of structural carbonate, possibly representing a lower need of adaptive strategies for survival in extreme cold. Increased mid-Holocene weathering of rock formations in the central mountains is suggested by sulfur isotope values. Scenarios related to water quality problems stemming from increased weathering, and a possibility of a catastrophic starvation event as a cause of, or contributing factor in their demise are discussed.

1. Introduction

The extinction of the woolly mammoth (*Mammuthus primigenius*) and the ice age megafauna in general have inspired an impressive body of literature discussing the relative importance of different possible contributing agents, with environmental change and humans as the foremost contenders (e.g. Bartlett et al., 2016; Graham et al., 2016; Kuzmin, 2010; Lorenzen et al., 2011; MacDonald et al., 2012; Nikolskiy and Pitulko, 2013; Nikolskiy et al., 2011; Nogués-Bravo et al., 2008; Stuart, 2005). While final consensus on the cause of extinction has not been reached, the spatiotemporal pattern of woolly mammoth distribution dynamics is well understood based on extensive compilations of radiocarbon (^{14}C) dated occurrence records for the species (e.g. MacDonald et al., 2012; Markova et al., 2013) and genetic studies providing estimates of effective population sizes and turn-overs (e.g. Barnes et al., 2007; Fellows Yates et al., 2017; Palkopoulou et al., 2013). After a period of range contraction and fragmentation, the last occurrences of the woolly mammoth are recorded at ~11 ka[1] in northern mainland Siberia and ~13 ka in northeastern North America (Guthrie, 2006; Nikolskiy et al., 2011; Stuart, 2015), but the

* Corresponding author.
E-mail addresses: laura.arppe@helsinki.fi (L. Arppe), juha.karhu@helsinki.fi (J.A. Karhu), sergey-vartanyan@mail.ru (S. Vartanyan), dorothee.drucker@ifu.uni-tuebingen.de (D.G. Drucker), heli.etu-sihvola@helsinki.fi (H. Etu-Sihvola), herve.bocherens@uni-tuebingen.de (H. Bocherens).

[1] ka is used to designate calendar ages in thousands of years.

https://doi.org/10.1016/j.quascirev.2019.105884

species survived into the Holocene on islands in the Bering and Chukchi Seas (Guthrie, 2004; Vartanyan et al., 1993).

The last surviving population of woolly mammoths found refuge on Wrangel Island, currently ca. 140 km off the coast of the Chukotka mainland in northeastern Siberia (Fig. 1). During the terminal Pleistocene lowstand of the global sea level, the area encompassing present-day Wrangel Island was a part of Beringia - an ancient landmass extending from Yakutia to Canada connected by the Bering Land Bridge, much of which is presently submerged in the Arctic and Bering Seas. At the end of Pleistocene, global sea level transgression gradually isolated Wrangel Island from the mainland and broke up Beringia. The final separation is estimated to have taken place at ca. 10.5–10 ka (Arppe et al., 2009; Manley, 2002; Saarnisto and Karhu, 2004; Vartanyan et al., 2008). After an initial phase during which the early Wrangel Island comprised extensive parts of the now inundated shelf, the island reached its present-day extent by 8 ka (Arppe et al., 2009).

Mammoths persisted on Wrangel Island for several thousands of years after extirpation on the mainland. Radiocarbon dating on a molar retrieved from the island currently places the last recorded occurrence of the species at ~4 ka (Ua-13366: 3685 ± 60 ^{14}C BP; Vartanyan et al., 2008). While extensive compilations of woolly mammoth distribution (MacDonald et al., 2012; Nikolskiy et al., 2011) reflected by densities of radiocarbon dates on the species have illustrated a pattern of prolonged decline on the mainland, with increasingly restricted distributions and sparser numbers of occurrence towards the end of the Pleistocene, the woolly mammoth record on Wrangel Island ends rather abruptly, without signs of prior decline of the population. The reason for the seemingly abrupt final demise of the Wrangel Island mammoth population is unresolved. Evidence of human activity on the island is limited to a single archaeological site, Chertov Ovrag, on the southern coast. It represents a Paleo-Inuit culture camp site, used for hunting marine mammals and geese (Bronshtein et al., 2016; Gerasimov et al., 2006). Chronologically the estimated use of the site between 3650 and 3350 cal BP (Bronshtein et al., 2016) postdates the last mammoth date (2σ age range 4224–3852 cal yr BP) by a minimum of 200 years. Palynological and isotopic evidence from Wrangel Island suggest that present day–like climatic conditions and floral composition were established right after the Pleistocene-Holocene transition, with no indication of further perturbations during the Holocene (Karhu et al., 1998; Lozhkin et al., 2011, 2001; Saarnisto and Karhu, 2004). Similarly, any significant reductions to the size of the foraging area available to the Wrangel Island mammoths had taken place by 8 ka (Arppe et al., 2009).

While proxy records of external factors have not been able to present a robust explanation to the demise of the Wrangel Island population, recent genetic studies have shed light on internal factors that have possibly made the population more vulnerable to extinction. Results from both mitochondrial DNA and nuclear genome-wide sequencing studies showed a drastic, at least 10-fold reduction in the effective population size of woolly mammoths following deglaciation (Palkopoulou et al., 2015, 2013). In addition, a severe loss of genetic diversity in the island dwelling mammoths was observed, an expected signal consistent with inbreeding in a small population of animals (Palkopoulou et al., 2015). A further analysis of the genome-wide data of one Wrangel Island mammoth dated to 4.3 ka revealed an accumulation of detrimental mutations (Rogers and Slatkin, 2017). Compared to a ~40 ka old Siberian counterpart, the Holocene island individual showed a greater number of gene deletions, premature stop codons and retrogenes which, although not lethal, may have added burden on the survival capacity of an already struggling population (Rogers and Slatkin, 2017). Interestingly, many of the excess gene deletions were related to metabolism. This raises an interesting question of

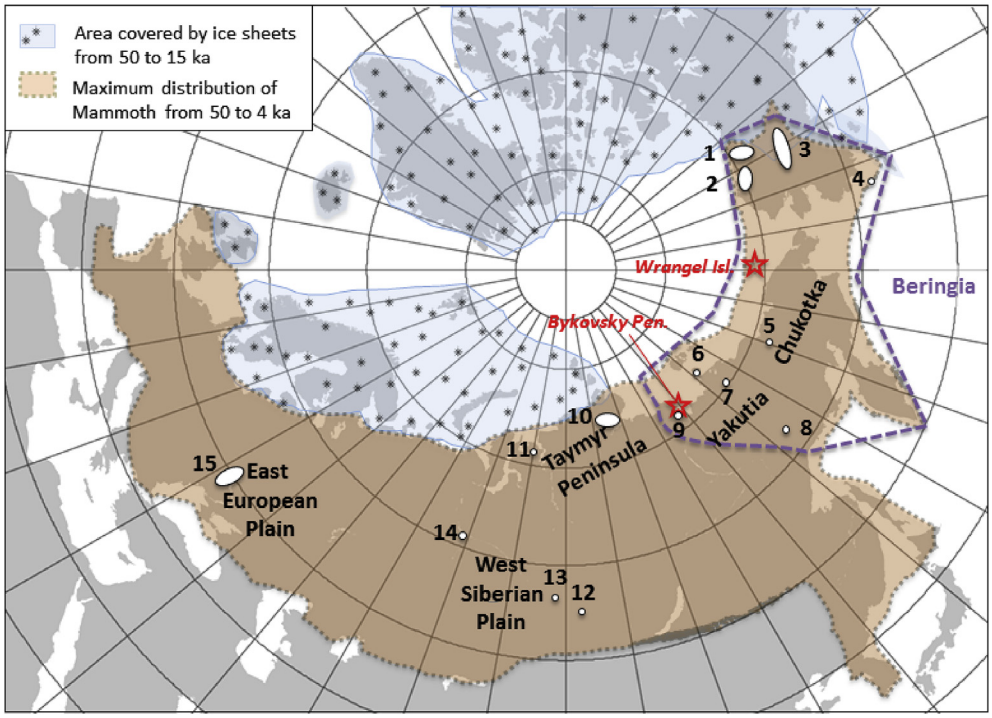

Fig. 1. Map showing the locations of mammoth materials discussed in this study. Stars indicate sites for material analysed in this study, Wrangel Island and Bykovsky peninsula. Circles indicate sites/regions mentioned in the text and Appendix of literature data. Key for site/region numbers: 1. Northern Yukon, 2. Northern Alaska, 3. Central Alaska and Yukon, 4. St. Paul Island, 5. Anyui River, 6. Bol'shoy Lyakhovsky Island, 7. Berelekh, 8. Omyakon, 9. Lena River Delta, 10. Taymyr Peninsula, 11. Gydan Peninsula, 12. Afontova Gora 2, 13. Krasnoyarska Kurya, 14. Lugovskoye, 15. East European Plain sites.

whether the Wrangel Island mammoth population differed from the ice age mainland animals in terms of their nutrition and metabolic functioning.

Apart from genetic methods, an independent and complementary view into the internal factors of mammoth 'well-being' is provided by the stable isotope compositions of their tissues. Isotope values of carbon ($\delta^{13}C$) and nitrogen ($\delta^{15}N$) in animal bones and teeth reflect the isotopic composition of the dietary input. Within the body, these are further modified by isotopic fractionation during metabolic reactions (DeNiro and Epstein, 1981, 1978). They can provide information pertaining to the habitat, e.g. temperature, moisture status, the type and quality of forage accessible and selected (Heaton, 1987; Iacumin et al., 2005; Mann et al., 2013), as well as the internal processing of energy and nutrients within the animal (Ambrose and DeNiro, 1986; Hatch, 2012; Sealy et al., 1987; Sponheimer et al., 2003). Previous isotopic studies on the woolly mammoths of North America and Eurasia have reported on a peculiar feature: their $\delta^{15}N$ values are consistently 3–6‰ higher than those of sympatric herbivores like reindeer and horse, on par with values characteristic for carnivores (Bocherens et al., 1994; Drucker et al., 2015; Fox-Dobbs et al., 2008; Iacumin et al., 2000). Several possible mechanisms for the characteristic isotopic signature of distinctly high $\delta^{15}N$ values, usually accompanied with low $\delta^{13}C$ levels have been discussed, related to a high level of dietary specialization (Drucker et al., 2018; Schwartz-Narbonne et al., 2015), distinct metabolic characteristics and special adaptive strategies of nutrient and energy recycling (Bocherens, 2003; Clementz et al., 2009; van Geel et al., 2011).

Changes in the isotopic composition of herbivores can document decreases of the ecological suitability of areas through time. For instance, a pattern of anomalously low woolly mammoth $\delta^{15}N$ values at Mezhyrich, Ukraine, dating to the post-glacial time ca. 18.5–17 ka shortly before the local extirpation of the species (17–14 ka; Stuart, 2005) was first reported by Drucker et al. (2014) and later observed at other contemporaneous sites of the East European Plain (Drucker et al., 2018; see Appendix B). The low $\delta^{15}N$ values, at the level or below those of coeval horses, were interpreted to reflect a population under environmental stress due to a loss of their accustomed ecological niche and thus, as a sign of increased vulnerability prior and perhaps linked to local extirpation.

In this study, we report on the isotopic compositions of carbon, nitrogen and sulfur in collagen of the world's last population of woolly mammoths on Wrangel Island. Our primary aim is to evaluate whether the animals were subsisting outside of their accustomed, optimal ecospace characterized by high $\delta^{15}N$ (and low $\delta^{13}C$) values. We compare the isotopic values of the Wrangel post-isolation, i.e. Holocene, mammoths to those of their ice-age mainland forebears to determine whether their nitrogen isotope values were lower, as reported for the pre-extinction population of the East European Plains, and potentially indicative of population stress and decline. Furthermore, we draw together all the currently available isotope records on the Wrangel Island mammoths in an attempt to arrive at an integrative picture of their Holocene existence on the island.

2. Material and methods

2.1. Large herbivore specimens

The skeletal material from Wrangel Island (Fig. 1) was collected from the banks of major rivers, as well as beach, slope and alluvial fan deposits during field expeditions between 1991 and 2000. A total of 60 specimens were sampled, representing mainly woolly mammoth (*Mammuthus primigenius*; $n = 52$), but also samples of muskox (*Ovibos moschatus*; $n = 6$) and bison (*Bison priscus*; $n = 2$) were included. As a reference point to the insular population, a set ($n = 31$) of mainland large herbivores from the Bykovsky peninsula (Fig. 1.), northern central Siberia (Yakutia), were sampled. These comprised 25 specimens of woolly mammoth and 6 of horse (*Equus caballus*). All non-modern specimens have been radiocarbon dated in prior studies (Nikolskiy et al., 2011; Schirrmeister et al., 2002; Sher et al., 2005; Vartanyan et al., 2008). Details of all the specimens and their respective dating information are given in Appendix A. The finite dates of the mammoth specimens from Wrangel Island span from ca. 42 to 4 ka. The musk oxen and bison range in age from recent to 23 ka. The Bykovsky peninsula mammoths show dates from ca. 48 to 17 ka, and the horse from 40 to 28 ka. Five mammoth specimens, two from Wrangel and three from Bykovsky peninsula, three musk oxen and one horse have infinite ^{14}C dates. See section 2.3 below for details on calibration of radiocarbon dates.

2.2. Isotopic and elemental analyses

For isotopic analyses of carbon, nitrogen and sulfur in collagen ($\delta^{13}C_{COLL}$, $\delta^{15}N_{COLL}$ and $\delta^{34}S_{COLL}$, respectively), a piece of bone or, in the case of tusk and molar specimens, dentine weighing 0.5–1 g was cut off. After rinsing in acetone and MilliQ-water, and drying, the pieces were manually crushed to powder. As a preliminary screening for the level of preservation, the contents of carbon, nitrogen and sulfur in the powdered bone/dentine were determined using a CNS elemental analyzer Vario EL III at the University of Tübingen. The collagen extraction was performed following Bocherens et al. (1997). Shortly, sample powders were demineralised in 1 M HCl for 20 min. After filtration, the samples were treated with 40 ml of 0.125 M NaOH solution in room temperature for 20 h. The solid phase was dissolved in pH 2 HCl solution at 100 °C, and the final filtrate was freeze-dried.

The quality of the collagen extracts was evaluated using established criteria. C/N ratios from 2.9 to 3.6 were considered indicative of well-preserved collagen (Ambrose, 1990; DeNiro, 1985; DeNiro and Weiner, 1988; Sealy et al., 2014; van Klinken, 1999). The acceptable range of carbon and nitrogen content is less precisely defined. Nitrogen contents of ca. 11–17% have been reported for fresh or well-preserved collagen (Ambrose, 1990; Sealy et al., 2014; van Klinken, 1999). For carbon, van Klinken (1999) gives a mean C% of 34.8 ± 8.8 in a large set of acceptable collagens, while higher values of 41–47% were suggested by Ambrose (1990) and Sealy et al. (2014). For sulfur, concentrations in collagen from 0.12 to 0.35%, and C/S ratios of 600 ± 300 and N/S ratios of 200 ± 100 are considered acceptable based on compositions of modern mammalian collagen (Bocherens et al., 2015, 2011; Nehlich and Richards, 2009).

The analysis of the weight-% and isotopic composition of carbon, nitrogen and sulfur in the extracted collagen was performed at the Department of Geosciences of the University of Tübingen (Germany), on an NC2500 elemental analyzer coupled to a Thermo Quest Delta + XL isotope ratio mass spectrometer. Measured data were calibrated to the recognized values of international reference materials and in-house reference materials, using a two-point (for $\delta^{13}C_{COLL}$ and $\delta^{15}N_{COLL}$) or multi-point calibration scheme. For $\delta^{13}C_{COLL}$ and $\delta^{15}N_{COLL}$ an in-house acetanilide material ($\delta^{13}C$ −30.0‰; $\delta^{15}N$ −1.0‰), USGS-24 ($\delta^{13}C$ −16.0‰) and IAEA-N-2 ($\delta^{15}N$ +20.3‰) were used. For $\delta^{34}S_{COLL}$ the calibration was based on NBS-123 (+17.10‰), IAEA-S-1 (−0.30‰) and IAEA-S-3 (−32.1‰). The calibration references indicate an internal precision (SD, 1σ) of ±0.1‰ for $\delta^{13}C$, ±0.2‰ for $\delta^{15}N$, and ±0.4‰ for $\delta^{34}S$. Additionally, collagens extracted alongside the samples from two in-house bone powders reference materials (camel and elk) were used to check for consistency of extraction, chemical composition and isotopic

composition among measurement series. The analyzed (n = 18) quality control materials indicate an external reproducibility (SD, 1σ) of ±0.1‰ for $\delta^{13}C_{COLL}$ values, ±0.2‰ for $\delta^{15}N_{COLL}$ and ±0.4‰ for the $\delta^{34}S_{COLL}$ values, consistent with that derived from calibration reference reproducibility. As a measure of accuracy, the two in-house collagen reference materials (n = 9 + 9) gave mean $\delta^{13}C_{COLL}$ values of −23.8 ± 0.1‰ and −14.8 ± 0.2 (expected: 23.9 ± 0.1‰ and −14.8 ± 0.15‰, respectively) and $\delta^{15}N_{COLL}$ values of 2.6 ± 0.2‰ and +8.0 ± 0.1‰ (expected: +2.7 ± 0.2‰ and +8.0 ± 0.2‰, respectively). All isotope data are given in the δ-notation as permil (‰), relative to the VPDB standard for carbon, AIR for nitrogen and CDT for sulfur.

Of the 52 woolly mammoth specimens from Wrangel Island, 50 samples have additional, previously determine but unpublished carbon isotope data for the structural carbonate of the bioapatite mineral ($\delta^{13}C_{CO3}$; see Appendix A). In case of molar specimens, the $\delta^{13}C_{CO3}$ value was determined for enamel, i.e. not the dentine tissue used for the analysis of collagen $\delta^{13}C_{COLL}$ value. The $\delta^{13}C_{CO3}$ values were determined at the Geological Survey of Finland, following the sealed vessel phosphoric acid method by McCrea (1950), with a reaction time of 1 h at 100 °C. Before the decarbonation reaction, the samples were treated 4 h to overnight with a 3% NaOCl solution in order to remove organic matter. The isotope ratios of carbon of the cryogenically purified CO_2 were measured on a Finnigan MAT 251 dual inlet mass spectrometer, using a CO_2 working gas standard calibrated relative to the VPDB reference standard using NBS-19. The external precision based on multiple sample measurements was 0.1‰. The accuracy estimate for the analyses is based on seven analyses of NBS-18 reference standard, analysed alongside unknowns, which yielded a $\delta^{13}C$ value of −5.01 ± 0.02‰, within the uncertainty range of the recommended value for NBS-18 (Coplen et al., 2006). The structural carbonate $\delta^{18}O$ values resulting from these analyses belong to another project and are not included in this paper.

2.3. Previously published isotope data

Some 38 of the Wrangel Island mammal specimens investigated for isotopic compositions of collagen in this study have a prior Sr-isotope ($^{87}Sr/^{86}Sr$) determination (Arppe et al., 2009; see Appendix A). As with the $\delta^{13}C_{CO3}$ analysis, the $^{87}Sr/^{86}Sr$ analysis was performed on enamel in case of molar specimens. The analytical methods and an in-depth discussion of the data were published by Arppe et al. (2009).

In addition to the above described Wrangel Island and Bykovsky peninsula datasets, stable isotope and dating data on woolly mammoths from Eurasia and northwestern North America were gathered from published literature to facilitate evaluation of large scale spatiotemporal patterns in mammoth diets, their habitats and success (Barbieri et al., 2008; Bocherens et al., 1994, 1996; Debruyne et al., 2008; Drucker et al., 2014, 2018; Graham et al., 2016; Grigoriev et al., 2017; Guthrie, 2004, 2006; Haesaerts et al., 2015; Holmes, 2011; Iacumin et al., 2010, 2000; Kirillova et al., 2015; Lanoë et al., 2017; Lanoë and Holmes, 2016; MacPhee et al., 2002; Mann et al., 2013; Metcalfe et al., 2016, 2010; Mol et al., 2001; Orlova et al., 2004; Palkopoulou et al., 2013; Pitulko et al., 2014; Kuzmin and Orlova, 2004; Poinar, 2006; Potter et al., 2013; Seuru et al., 2017; Stupak, 2014; Styring et al., 2015; Szpak et al., 2010; Veltre et al., 2008; Zolnikov et al., 2017). In Siberia, considerable isotopic datasets have accumulated especially for the Taymyr Peninsula and Yakutia regions. In North America, data focus on three larger areas: northern Alaska, northern Yukon and central Alaska&Yukon. Altogether, $\delta^{13}C_{COLL}$ and $\delta^{15}N_{COLL}$ values, and some additional $\delta^{13}C_{CO3}$, $^{87}Sr/^{86}Sr$ and $\delta^{18}O$ data, were retrieved for 178 dated specimens (Appendix B). Isotope data for a further 119 samples with no or infinite radiocarbon dates are also listed, but these are not included in analysis unless otherwise specified. The number of finitely dated samples with both $\delta^{13}C_{COLL}$ and $\delta^{15}N_{COLL}$ values was 49 for Siberia (n = 19/30 West of/East of 127°E), 77 for northwestern North America (n = 26/51 northern/central East Beringia) and 15 for Holocene island populations (n = 1/14 Wrangel/St. Paul Island). In addition to the data from these Arctic and insular reference populations, Appendix B lists isotope values for the terminal Pleistocene mammoths of the East European Plain referred to in the introduction (n = 32) and some other Russian lower-latitude specimens (n = 5).

The original reported (raw) ^{14}C dates were recalibrated using the online Calib Radiocarbon Calibration program (Stuiver et al., 2019) and the IntCal13 calibration dataset (Reimer et al., 2013). For specimens with a raw ^{14}C date beyond 46,400 ^{14}C yr BP, the current limit of the IntCal calibration, calendar-equivalent ages were estimated using the online version of the CalPal-2007 calibration program and the Hulu age model (Weninger et al., 2007; Weninger and Jöris, 2008). The calendar ages of specimens with finite ^{14}C dates above 50,000 ^{14}C yr BP, unattainable also by the Hulu age model, are discussed and plotted with an age of ~60 ka. Throughout the text, "infinite" is only used to refer to sample dates that have produced an inconclusive dating result, i.e. beyond the method limit which varies from laboratory to laboratory. If not otherwise mentioned, dates for specimens are discussed as median values of calibrated calendar age ranges before present, as thousands of years (ka).

2.4. Adjustment for atmospheric CO_2 changes

Comparisons of herbivore $\delta^{13}C$ data from before and after the last deglaciation interval necessitate consideration of changes that took place at the root of the carbon source - plants and atmospheric CO_2. An accumulating body of evidence suggests that atmospheric CO_2 had similar $\delta^{13}C$ values during the full glacial (>18 ka) and the pre-1950 CE Holocene (Eggleston et al., 2016; Lourantou et al., 2010; Schmitt et al., 2012). However, the significant increase in the partial pressure of CO_2 (pCO_2) over the deglaciation interval from ca. 18 to 12 ka appears to have resulted in a decline of $\delta^{13}C$ values of plants and animals feeding on them (Breecker, 2017; Hare et al., 2018; Hatté et al., 1998), although views altogether opposing a *p*CO2 influence (Kohn, 2016) or emphasizing the significance of differences in habitat openness (Drucker et al., 2008) draw attention to the likely complex, interconnected nature of forcing factors. In a recent examination combining high-resolution records of atmospheric CO_2, model predictions and ^{14}C dated proxy data on terrestrial carbon archives, Hare et al. (2018) suggest a mean CO_2-baseline induced offset of 0.5‰ in the $\delta^{13}C$ values of animals of Holocene (<10 ka) and glacial age (>20 ka). Here, we adopt the suggested adjustment of +0.5‰ for the $\delta^{13}C$ data of Holocene specimens dated to ≤12 ka, and leave the transition period (ca. 18−12 ka) specimens without adjustment. However, it should be stressed that the effects of changing *p*CO2 forcing on plant ^{13}C discrimination are still far from well understood, and it appears that plants might show different responses in circumstances of elevated versus low *p*CO2 (Zhang et al., 2019 and references therein). Thus it is possible that future research on this score calls for a re-evaluation of the approach chosen here. Advances in e.g. model predictions of ^{13}C discrimination by angiosperm plants in response to shifting levels of pCO_2 and pO_2 (Hare et al., 2018) will hopefully allow for more sophisticated baseline considerations.

2.5. Data-analysis

Differences in isotopic values between mammoth populations

from different regions and time periods were tested using statistical methods. We tested for differences in isotopic values between Wrangel Island and Bykovsky specimens, and between Wrangel Island samples pre- and post-dating the isolation of the island at ca. 12–10 ka. Due to our primary interest in the Holocene population on Wrangel Island, further comparisons of reference population datasets from Siberia (with the new Bykovsky peninsula data merged with literature data), North America and St. Paul Island were made against Wrangel isotope data dating to the island period, i.e. <10 ka. In addition to datasets of finitely dated north Alaskan and central Alaska/Yukon samples, comparisons were made to specimens from northern Yukon where all specimens are either undated or have yielded infinite dates.

It is generally recognized that sufficiently large datasets ($n > 30$) allow for the use of parametric statistical procedures without major problems even if the data are not normally distributed. Thus, a two-tailed Student's t-test (datasets with equal variance) or Welch's *t*-test (unequal variance) was used for comparisons between groups with $n > 30$. Variance was considered by a two-sample test for variance F-statistic. For groups with $n \leq 30$, a Shapiro-Wilks test was used to test for normality of data distribution and differences were studied with a Mann-Whitney test for non-normal data. Data analysis was done using OriginPro 2018b software, and reported differences were significant at the 95% level ($p < 0.05$).

3. Results

3.1. Isotopic integrity of samples

Collagen yields were above 6% (mean 15.7% ± 5.6) for all specimens, and the extracts showed C % (40–46.1%), N % (14.1–16.4%) and C/N ratios (3.1–3.4) comparable to the range of values characteristic for fresh specimens. The contents of sulfur ranged from 0.14 to 0.23%, and the C/S and N/S ratios were 473–872 and 145–269, respectively, all within ranges reported for fresh bone materials. This indicates good preservation of collagen, not surprising considering the extremely cold, dry Arctic climate and permafrost conditions of the area.

The $\delta^{13}C_{CO3}$ values of all except one (ARP-78) sample were assessed as well preserved. All samples produced consistent and expected CO_2 yields for biogenic hydroxyapatite and showed a spacing between the $\delta^{13}C_{CO3}$ and $\delta^{13}C_{COLL}$ values ($\Delta^{13}C_{CO3\text{-}COLL}$; range 7.8–11.4‰, mean 9.4‰ ± 0.7) in the range of previously reported $\Delta^{13}C_{CO3\text{-}COLL}$ offsets for woolly mammoths (Bocherens et al., 1994; Iacumin et al., 2010; Metcalfe et al., 2010). Tusk sample ARP-78 showed an aberrant $\Delta^{13}C_{COLL\text{-}CO3}$ offset (4.0‰), and its anomalously low $\delta^{13}C_{CO3}$ value (−18.3‰) was omitted from data analysis and discussion.

3.2. Isotopic values

The isotopic data for all the Wrangel Island and Bykovsky peninsula herbivore specimens are listed in Appendix A. The following ranges are for the unadjusted data describing all specimens, including those with infinite dates. The Wrangel mammoths yielded $\delta^{13}C_{COLL}$ values from −23.0 to −20.4‰, $\delta^{15}N_{COLL}$ values from +7.8 to +14.7‰ and $\delta^{34}S_{COLL}$ values from −3.3 to +11.4‰. Their $\delta^{13}C_{CO3}$ values ranged from −14.6 to −10.7‰. The mammoths from Bykovsky peninsula had $\delta^{13}C_{COLL}$ values from −22.2 to −20.6‰, $\delta^{15}N_{COLL}$ values from +7.4 to +13.4‰ and $\delta^{34}S_{COLL}$ values from +2.3 to +6.2‰.

The pre-modern musk-oxen ($n = 4$) from Wrangel Island showed $\delta^{13}C_{COLL}$, $\delta^{15}N_{COLL}$ and $\delta^{34}S_{COLL}$ values from −21.0 to −19.5‰, +1.8 to +7.9‰ and +0.1 to +4.0‰, respectively, while the recent samples had $\delta^{13}C_{COLL}$ values at −21.1 to −21.0‰, $\delta^{15}N_{COLL}$ values at +5.5 to +5.6‰ and $\delta^{34}S_{COLL}$ values at +4.3 to +7.1‰. The bison ($n = 2$) had corresponding values at −20.7 to −20.2‰, +8.6 to +10.4‰ and +3.6 to +3.7‰. The musk-oxen, thus, conform to the expected pattern of distinctly higher mammoth $\delta^{15}N_{COLL}$ values, but the two bison specimens show $\delta^{15}N_{COLL}$ values comparable to the mammoths'.

The horses ($n = 5$) from Bykovsky peninsula displayed $\delta^{13}C_{COLL}$ values from −21.8 to −20.2‰, $\delta^{15}N_{COLL}$ from +4.1 to +7.6‰ and $\delta^{34}S_{COLL}$ values from −1.9 to +7.3‰. Thus, they are consistent with the usual pattern of mammoths generally having $\delta^{15}N_{COLL}$ values 3–6‰ higher compared to sympatric horses.

3.2.1. Regional comparisons

Table 1 summarizes the mean isotope values and standard deviation for the pre-modern specimens with finite dates. In the following discussion, $\delta^{13}C$ data for samples with dates <12 ka include a +0.5‰ adjustment discussed above (Chapter 2.4). As a whole, the mammoth specimens from Wrangel Island showed $\delta^{34}S_{COLL}$ and $\delta^{13}C_{COLL}$ values similar to those of mammoths from the Bykovsky peninsula, but had significantly higher $\delta^{15}N_{COLL}$ values. The collagen and carbonate $\delta^{13}C$ values of specimens dating to the time period preceding the isolation of the island ($n = 11$) and those post-dating isolation (<10 ka; $n = 39$) were statistically the same. Post-isolation specimens had a lower mean $\delta^{15}N_{COLL}$ and a higher mean $\delta^{34}S_{COLL}$ value.

Comparisons of large-scale regional mean $\delta^{13}C_{COLL}$ and $\delta^{15}N_{COLL}$ values against the Wrangel Island Holocene mammoth population data are presented in Fig. 2. The Siberian reference dataset includes the new data from Bykovsky peninsula. Statistically significant differences from Wrangel Island data, indicated by an asterisk in Fig. 2, were observed for several reference populations. However, many of these statistical indications are not considered meaningful in terms of actual ecological differences as these offsets are smaller or equal to typical analytical reproducibility, or may be related to dataset composition (see discussion in sections 4.1.1 and 4.1.2; also Amrhein et al., 2019). In addition to northern Yukon, mammoth $\delta^{13}C_{COLL}$ and $\delta^{15}N_{COLL}$ values from Siberia (~60–12 ka) and $\delta^{13}C_{COLL}$ values from northern Alaska (~60–21 ka) show greatest similarity to Wrangel Island values. The largest differences to Wrangel Island mammoth data were displayed by the Holocene mammoths from St. Paul Island, which had the highest $\delta^{13}C_{COLL}$ values (−19.5‰ ± 0.7) and lowest $\delta^{15}N_{COLL}$ values (+6.5‰ ± 1.5) of all reference groups. Data numbers for $\delta^{13}C_{CO3}$ values of finitely dated specimens are relatively low for other reference populations, but the Holocene Wrangel Island mammoths display a significantly higher mean value (−12.0‰ ± 0.5) compared to that of Pleistocene Siberian ones (−14.0‰ ± 0.7) (Fig. 3).

4. Discussion

4.1. Wrangel Island $\delta^{13}C$ and $\delta^{15}N$ paleoecology

4.1.1. $\delta^{15}N$ values

Several earlier studies have commented on a tendency of mammoth tooth specimens, i.e. molars and tusks, to display higher $\delta^{15}N_{COLL}$ values than bones (e.g. Bocherens et al., 1997, 1994; Metcalfe et al., 2010) and the cause was speculated to be linked to lingering effects of milk consumption during the juvenile period. Indeed, observations of particularly high $\delta^{15}N_{COLL}$ values in second and third molars (Metcalfe et al., 2010), in development during the juvenile stage, are consistent with a nursing effect. At the same time systematically higher $\delta^{15}N_{COLL}$ values also in the fifth and sixth molars (Metcalfe et al., 2010) that develop during adulthood suggest additional, unknown mechanisms at the root of the phenomenon.

Table 1
Mean isotope values and SD for the pre-modern herbivore specimens with finite dates. Values in italics include a +0.5‰ adjustment of $\delta^{13}C$ values for samples with dates <12 ka (see section 2.4).

	$\delta^{13}C_{COLL}$	$\delta^{15}N_{COLL}$	$\delta^{34}S_{COLL}$	$\delta^{13}C_{CO3}$	$\Delta^{13}C_{CO3\text{-}COLL}$	n
Wrangel Island						
mammoth	−21.9 ± 0.5	+9.8 ± 1.2	+4.6 ± 2.9	−12.5 ± 0.7	9.4 ± 0.7	50
	−21.5 ± 0.4			*−12.1 ± 0.7*		
tusk	−22.2 ± 0.2	+9.4 ± 0.6	+7.3 ± 2.6	−12.3 ± 0.7	9.9 ± 0.7	8
	−21.7 ± 0.2			*−11.8 ± 0.7*		
molar	−21.9 ± 0.5	+10.0 ± 1.3	+4.3 ± 2.7	−12.4 ± 0.6	9.4 ± 0.6	37
	−21.5 ± 0.4			*−12.0 ± 0.6*		
bone	−22.0 ± 0.3	+9.2 ± 1.1	+2.5 ± 2.8	−13.4 ± 1.2	8.6 ± 0.9	5
pre-isolation	−21.5 ± 0.6	+11.7 ± 1.7	+1.9 ± 2.4	−12.4 ± 1.1	9.1 ± 0.8	11
post-isolation	−22.1 ± 0.3	+9.4 ± 0.6	+5.4 ± 2.6	−12.5 ± 0.5	9.5 ± 0.6	39
	−21.6 ± 0.3			*−12.0 ± 0.5*		
bison, *bone*	−20.5 ± 0.2	+9.5 ± 0.9	+3.7 ± 0.0	–	–	2
musk oxen, *bone*	−19.5	+5.3	+0.1	–	–	1
Bykovsky peninsula						
mammoth	−21.4 ± 0.4	+8.9 ± 1.3	+4.2 ± 1.1	–	–	22
tusk	−21.0 ± 0.4	+11.2 ± 2.5	+5.2 ± 0.8	–	–	3
bone	−21.5 ± 0.3	+8.6 ± 0.5	+4.0 ± 1.1	–	–	19
horse, *bone*	−21.1 ± 0.6	+5.2 ± 1.4	+4.4 ± 3.6	–	–	5

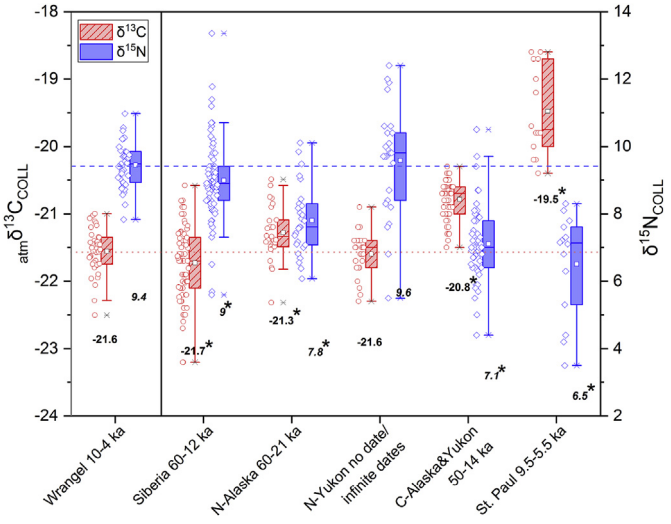

Fig. 2. Regional differences in $\delta^{13}C_{COLL}$ and $\delta^{15}N_{COLL}$ values. Whiskers mark the min-max range of continuous data (1.5 coefficient). Box borders represent 25% and 75% quartiles, the horizontal line shows the median. Dataset mean is marked by the white rectangle symbol within the box and written out below the data. An asterisk* next to the regional mean value indicates a statistically significant difference to Wrangel Island data. Note: the $\delta^{13}C_{COLL}$ values were adjusted for the atmospheric CO_2 effect (see section 2.4) but the $\delta^{15}N_{COLL}$ values are **not** adjusted for any possible tissue-effect discussed in section 4.1.1. "Siberia 60–12 ka" includes data from Taymyr Peninsula and Yakutia (Fig. 1; Appendix B).

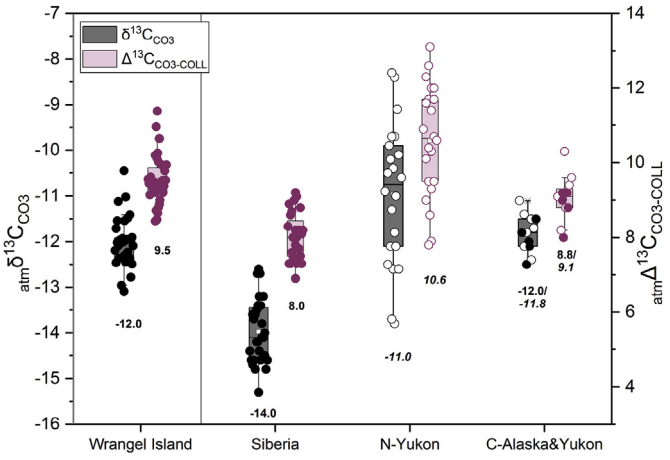

Fig. 3. Comparison of regional $\delta^{13}C_{CO3}$ and $\Delta^{13}C_{CO3\text{-}COLL}$ values. $\delta^{13}C_{CO3}$ values for samples with ages <12 ka were adjusted +0.5‰ for the atmospheric CO_2 effect (see section 2.4). Filled symbols denote data for samples with finite dates, unfilled symbols are for samples with unknown ages. Box and whisker statistics as in Fig. 2, drawn for all data for central Alaska&Yukon. Mean values (*italics*: samples with unknown ages included) are displayed below boxes. Data is not available for northern Alaska or St. Paul Island.

A comparison of mean $\delta^{15}N_{COLL}$ values according to anatomical part (Table 2) of the data compiled in Appendix B and the new data from this study further shows that the mammoth dental ^{15}N bias is a robust and pervasive phenomenon: compared to bone $\delta^{15}N_{COLL}$ values on a regional basis, teeth (molar and tusk samples combined) show 0.7–2.6‰ higher mean values. Despite the current lack of knowledge of the reasons and the exact magnitude of the effect, it is evident that comparisons of datasets that are very unbalanced in terms of anatomical composition are susceptible to tissue type induced errors, i.e. datasets that have a higher contribution of molar and tusk samples are likely to yield higher mean $\delta^{15}N_{COLL}$ levels.

Tooth specimens make up 90% of all the mammoth material for Wrangel Island in this study, and 94% of the post-isolation dataset. It is therefore likely that the significantly higher $\delta^{15}N_{COLL}$ value of Wrangel island mammoths in comparison to those from the Bykovsky peninsula, the Siberian mammoths as a whole, and to some extent also for north Alaska (Fig. 2), is due to the fact that the relative proportion of teeth in these mainland reference datasets is much lower (Bykovsky and Siberia 13–14%, north Alaska 28%; Table 2). In contrast, the northern Yukon dataset with high $\delta^{15}N_{COLL}$ values, statistically the same as those of Wrangel Island, also has a very similar anatomical makeup with an 88% share of tooth samples. Like for Wrangel Island, the dataset for St. Paul Island is also heavily biased towards tooth specimens (93%), and there is no cause to suspect that the significantly lower $\delta^{15}N_{COLL}$ values from St. Paul are an artefact of sample type differences. A rigorous evaluation of the anatomical comparability of the central East Beringian dataset is somewhat hindered by the ten specimens with no anatomical assignment (Appendix B). However, excluding data for these samples leads to no change in the regional mean $\delta^{15}N_{COLL}$ value (+7.1‰, Fig. 2) and a dataset with 52% teeth, which again suggests that part of the higher mean $\delta^{15}N_{COLL}$ value for Wrangel Island might be attributable to the higher proportion of teeth. In

Table 2
Mean $\delta^{15}N$ values by anatomical part type, the difference to bone values (*diff.*), and the proportion (%) of tooth and bone specimens in the dataset. For values in bold *n* is less than 5, underlined values in bold indicate cases where n = 1. Unidentified anatomical parts from central (n = 9) and northern Alaska (n = 1), and central Yukon (n = 1) were not included in the comparison. Siberia includes the new data from Bykovsky peninsula, and literature data from Taymyr Peninsula, Yakutia and Chukotka. Wrangel data include an additional bone sample from an earlier study. See Appendix B.

	$\delta^{15}N$, finite dates (‰)				Teeth	Bone	$\delta^{15}N$, ALL samples (‰)				Teeth	Bone
	Molar	Tusk	Tooth	Bone	%	%	Molar	Tusk	Tooth	Bone	%	%
Wrangel	+10.0	+9.4	+9.9	+9.1	90	10	+9.9	+9.4	+9.8	+9.1	90	10
diff.	*0.9*	*0.3*	*0.8*	–			*0.8*	*0.3*	*0.7*		–	
Wrangel <10ka	+9.4	+9.4	+9.4	**+8.2**	94	6	–	–	–	–		
diff.	*0.9*	*0.3*	*0.8*	–			–	–	–	–		
Bykovsky peninsula	–	**+11.2**	**+11.2**	+8.6	14	86	–	**+11.2**	**+11.2**	+8.6	16	84
diff.	–	*2.6*	*2.6*	–			–	*2.6*	*2.6*	–		
Siberia	**+9.6**	+10.3	+10.1	+8.8	13	87	**+9.8**	+10.4	+10.2	+9.2	9	91
diff.	*0.7*	*1.5*	*1.3*	–			*0.6*	*1.2*	*1.0*	–		
North Alaska	+9.0	**+7.7**	+8.6	+7.5	28	72	+8.8	+7.8	+8.5	+7.4	51	49
diff.	*1.4*	*0.2*	*1.1*	–			*1.4*	*0.4*	*1.1*	–		
North Yukon	–	–	–	–			+9.9	–	+9.9	**+7.5**	88	12
diff.	–	–	–	–			*2.4*	–	*2.4*	–		
Central Alaska	+6.8	**+7.3**	+6.8	**+5.8**	95	5	+6.9	+7.2	+6.9	**+5.8**	95	5
diff.	*1.0*	*1.5*	*1.0*	–			*1.1*	*1.4*	*1.1*	–		
Central Yukon	**+8.0**	–	+8.0	+7.3	14	86	+8.0	–	+8.0	+7.3	25	75
diff.	*0.7*	–	*0.7*	–			*0.7*	–	*0.7*	–		
St.Paul Island	+6.4	**+7.3**	+6.8	**+5.3**	93	7	–	–	–	–		
diff.	*1.1*	*2.0*	*1.5*	–			–	–	–	–		
East European plain	+7.7	**+6.2**	+7.5	+5.5	34	66	–	–	–	–		
diff.	*2.2*	*0.7*	*2.0*	–			–	–	–	–		

summary, taking into account different proportions of hard tissue types within the isotopic datasets, we conclude that the $\delta^{15}N_{COLL}$ values of Holocene mammoths on Wrangel Island were very similar to those of other Beringian mammoths indicating ecological comparability. It's however likely that a lower mean $\delta^{15}N_{COLL}$ value for the mammoths of central East Beringia, earlier discussed by Szpak et al. (2010), persists even after inter-tissue variability considerations. The conspicuously low $\delta^{15}N_{COLL}$ values (Fig. 2) of the St. Paul mammoth population as compared to Wrangel Island represent a real difference in the isotopic baselines, dietary composition and/or metabolic processing of diet of these two late surviving island populations.

A more detailed analysis of the tissue bias phenomenon, carefully taking into account the spatiotemporal variability in nitrogen isotopic baselines and preferably also the pre-/post-weaning formation of different tooth samples, is needed before a suitable correction factor (or factors) can be inferred. Such an analysis is beyond the scope of this paper, but to enhance the comparability of the $\delta^{15}N_{COLL}$ records in Figs. 4 and 5, showing the compiled mammoth $\delta^{13}C_{COLL}$ and $\delta^{15}N_{COLL}$ values as a function of time we took the mean value, amounting to 1‰ (±0.6), of all the calculated regional tooth-bone offsets (Table 2) and adjusted the tooth $\delta^{15}N_{COLL}$ data down to a "bone-equivalent" level. An unadjusted version of Fig. 4 is provided as a supplementary file (Suppl. Fig. 1).

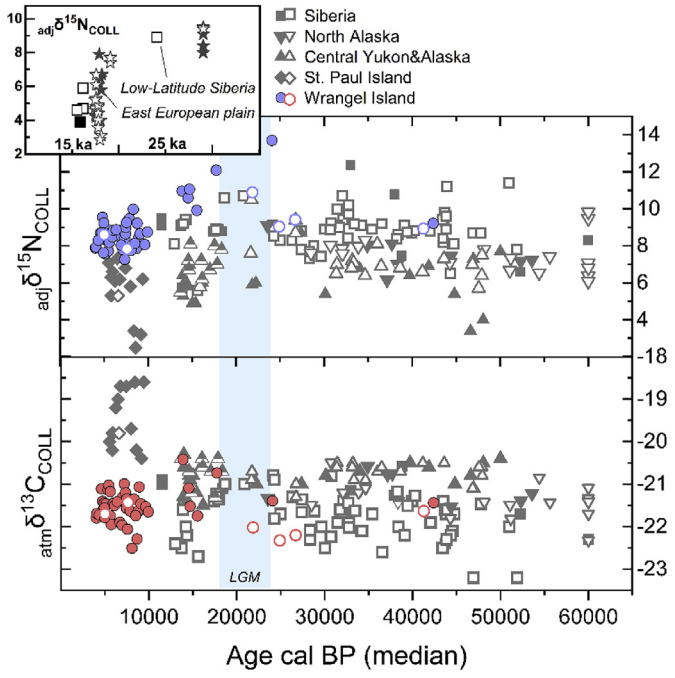

Fig. 4. $\delta^{13}C$ and $\delta^{15}N$ values for Beringian woolly mammoths. $\delta^{13}C$ values for samples with calendar ages <12 ka have been adjusted +0.5‰ for changes in atmospheric CO_2 (see section 2.4). $\delta^{15}N$ values of tooth specimens have been adjusted −1‰ to account for systematic tissue related offset (see section 4.1.1). Solid symbols show data for teeth, open symbols for bone specimens. Half-filled symbols indicate specimens without anatomical identification. Finite ^{14}C dates >50 ka, beyond current calibration curves, are plotted at 60 ka. Inset shows $\delta^{15}N$ values of low-latitude mammoths from the East European plain (stars) and Southern/central Siberia (squares). Data for all plotted samples (n = 250) are listed in Appendices A and B.

4.1.2. $\delta^{13}C$ values

The *t*-test indicated that the mean $\delta^{13}C_{COLL}$ value for the Holocene Wrangel Island mammoths was significantly different from that of all other regions except north Yukon. Considering typical measurement uncertainties, inter-laboratory differences, intra-skeleton variation and the approximate nature of the applied +0.5‰ atmospheric adjustment of $\delta^{13}C_{COLL}$ values, we do not consider the differences shown against Siberian (0.1‰) and north Alaskan (0.3‰) data meaningful nor indicative of dissimilarities in the diets or habitats of the animals. The offsets in $\delta^{13}C_{COLL}$ values between Wrangel Island and central East Beringian (0.8‰) and St. Paul (2.1‰) mammoths, however, are taken to represent differences in some aspects of the dietary ecology of the populations – either in the isotopic baseline levels affected by e.g. climate or soil properties, food availability and/or metabolic processing.

The pool of comparison data is more limited for $\delta^{13}C$ values of structural carbonate (Appendix B), but an intriguingly contrasting pattern is observed for the $\delta^{13}C_{CO3}$ values and calculated $\Delta^{13}C_{CO3-}$

COLL offsets displayed in Fig. 3. In comparison to Siberia (−14.0‰ ± 0.7, n = 28), northern Yukon (−11.0‰ ± 1.5, n = 22, no/infinite dates) and central East Beringia (−12.0‰ ± 0.4, n = 5), the post-isolation Wrangel Island $\delta^{13}C_{CO3}$ values (−12.0‰ ± 0.5, n = 36) are closest to those of central East Beringia. Increasing data numbers by incorporating also the samples of unknown age for central East Beringia results in very little change in the mean $\delta^{13}C_{CO3}$ (−11.8‰ ± 0.4, n = 12). The $\delta^{13}C$ value of collagen is more influenced by dietary protein, but in contrast, the $\delta^{13}C_{CO3}$ value follows the composition of blood bicarbonate (e.g. Passey et al., 2005) and reflects the total carbon input (carbohydrates, lipids, proteins) of an animal's diet (Ambrose and Norr, 1993; Jim et al., 2004; Tieszen and Fagre, 1993). Two mechanisms are likely to play a role in the variation observed in animal $\Delta^{13}C_{CO3\text{-}COLL}$ values. The first mechanism is linked to dietary use of lipids. Indeed, increased proportions of energy received as lipids lead to lower $\delta^{13}C_{CO3}$ values, and hence, lower $\Delta^{13}C_{CO3\text{-}COLL}$ due to the generally low $\delta^{13}C$ values of fats (DeNiro and Epstein, 1978; O'Connell and Hedges, 2017; Tieszen et al., 1983). A second, alternative or complementary mechanism is related to microbial fermentation of dietary fibers. When this process increases, higher $\delta^{13}C_{CO3}$ values, and associated larger $\Delta^{13}C_{CO3\text{-}COLL}$, occur via loss of ^{13}C depleted CH_4 and possible reuse of ^{13}C enriched CO_2 formed in the gut (Codron et al., 2018; Hedges, 2003; Tejada-Lara et al., 2018).

The closer similarity in $\delta^{13}C_{CO3}$ and $\Delta^{13}C_{CO3\text{-}COLL}$ values between Wrangel and East Beringian, i.e. northern Yukon, central Alaska and central Yukon, mammoths (Fig. 3) could be linked to the consumption of forage with similar non-proteinaceous qualities. Interestingly, paleovegetation in the first part of the Holocene on Wrangel Island shows a greater affinity to Eastern Beringia than the geographically closer Western Beringia as indicated by pollen analysis (Lozhkin et al., 2001), which may explain the similar $\delta^{13}C_{CO3}$ patterns of mammoths from these areas. Data numbers and chronological control are perhaps still suboptimal for the mammoths of East Beringia, but the dataset for Siberian mammoths seems sufficient for a representative estimate of regional $\delta^{13}C_{CO3}$ levels. The Holocene Wrangel Island mammoths show 2‰ higher values compared to Siberian ones, a difference clearly beyond possible analytical or correction factor issues. The above discussion of likely tissue bias in $\delta^{15}N_{COLL}$ values raises concerns of a similar effect for carbon. Systematically higher (or lower) $\delta^{13}C$ values in mammoth tooth versus bone collagen have not been reported. An examination of the effects of nursing in woolly mammoths suggested decreased, not increased, $\delta^{13}C$ values of collagen (~0.2‰) and structural carbonate (~2‰) (Metcalfe et al., 2010). Thus, a postulated larger share of juvenile molars in the tooth-heavy Wrangel Island dataset should actually bias the dataset towards lower, not higher, values. Thus, we consider the differences in $\delta^{13}C_{CO3}$ and $\Delta^{13}C_{CO3\text{-}COLL}$ values between these two mammoth populations as a sign of real differences in dietary ecology. According to the current paradigm, the higher $\delta^{13}C_{CO3}$ values of the Wrangel Island population could be interpreted as a higher level of CH_4 formation during digestion, or/and less reliance on ^{13}C depleted fat reserves than for the Siberian Pleistocene mammoths.

4.1.3. Summarizing regional $\delta^{13}C$ and $\delta^{15}N$ records

The Wrangel Island $\delta^{13}C_{COLL}$ and $\delta^{15}N_{COLL}$ data are placed within their temporal context with other Beringian mammoth records in Fig. 4. The Holocene $\delta^{13}C_{COLL}$ and $\delta^{15}N_{COLL}$ levels of the Wrangel Island mammoths appear as a natural continuation of Pleistocene Siberian mammoth isotope values and indicate a comparable feeding ecology especially in terms of dietary proteins. Summarizing the current understanding of the diets of Siberian and East Beringian mammoths alike, they were likely based on plants with relatively high $\delta^{15}N$ values, like old growth and snow buried, partly decayed grasses, graminoids and herbs, growing in dry, possibly trampled and dung-fertilized habitats (Bocherens, 2003; Bocherens et al., 1996; Mann et al., 2013; Schwartz-Narbonne et al., 2015; Szpak et al., 2010), possibly supplemented by coprophagy (van Geel et al., 2011). With reference to the major motivation of this study, the observation of low $\delta^{15}N_{COLL}$ levels in the pre-extinction mammoths of the East European Plains and also those of lower latitude Siberia (Appendix B and inset in Fig. 4) as a sign of population stress and decline before local extinction (Drucker et al., 2018, 2014), such a phenomenon is not observed among Wrangel Island mammoths. The higher pre-isolation mean $\delta^{15}N_{COLL}$ value of the Wrangel Island mammoths (Results, section 3.2.1) compared to the post-isolation island population on Wrangel is caused by the few peak values relating to the LGM perturbation (see below), and does not represent a difference in pre-to post-isolation dietary ecology.

The combination of similar $\delta^{13}C_{COLL}$ values and clearly higher $\delta^{13}C_{CO3}$ values in the Wrangel mammoths compared to their Siberian predecessors are suggestive of differences in the energy (lipids + carbohydrates) component of their dietary ecology. A higher reliance on ^{13}C depleted bodily fat reserves in the Pleistocene Siberian mammoths (Bocherens et al., 1996; Iacumin et al., 2000; Szpak et al., 2010) seems plausible considering the ameliorated climatic conditions for the Holocene mammoths on Wrangel Island compared to the Pleistocene Siberian ones. It is inviting to draw a speculative link from the possibly decreased need of bodily reserve fat storage in the Wrangel mammoths to the gene deletions of lipocalins − proteins associated with the transport of hydrophobic molecules like lipids, steroids, carotenoids in the body − reported by Rogers and Slatkin (2017) among the detrimental mutations for the Wrangel mammoth. The higher $\delta^{13}C_{CO3}$ levels could also be related to more CH_4 formation in the digestion process, e.g. due to more fibrous diets for the Wrangel Island mammoths. We additionally note, that the lowest $\delta^{13}C_{CO3}$ values of all the Wrangel Island specimens date to 27–22 ka (Fig. 5), just prior to and during the LGM, supporting a link between generally harsher conditions and lowered $\delta^{13}C_{CO3}$ values.

The stable isotope record is sparse over the peak cold conditions of the Last Glacial Maximum, ca. 24–18 ka, reflecting the overall decline and post-LGM recovery of northern mammoth populations (MacDonald et al., 2012). The lowest regional $\delta^{13}C_{COLL}$ values and highest $\delta^{15}N_{COLL}$ values were reported for LGM specimens in central East Beringia (Szpak et al., 2010). Similarly on Wrangel Island, the lowest $\delta^{13}C_{CO3}$ and highest $\delta^{15}N_{COLL}$ values are displayed right before and after the LGM (Fig. 5). These signals can be interpreted as a combined response of plants to extreme aridity (Craine et al., 2009; Heaton, 1987; Murphy and Bowman, 2006) and increased internal recycling of energy reserves and tissues in the mammoth body (Bocherens, 2003; Doi et al., 2017; Szpak et al., 2010). However, there seems to be no consistent response to the extremely cold conditions across Beringia.

From the viewpoint of isotopic values of collagen, the ecologies of the two Beringian mammoth populations surviving in insular conditions into the Holocene are very different. The distinctly higher $\delta^{15}N_{COLL}$ and lower $\delta^{13}C_{COLL}$ values of the Wrangel Island mammoths can, partly if not wholly, be related to large scale latitudinal trends in temperature and precipitation affecting isotopic baselines at the plant level (Craine et al., 2009; Kohn, 2010), i.e. much more arid and colder conditions on Wrangel Island compared to St. Paul, situated 1600 km to the southeast. The high $\delta^{13}C_{COLL}$ values of the St. Paul mammoths are an outstanding feature among Beringian mammoth isotope records (Fig. 4). Compared to the isotopically most similar mammoths of central East Beringia, St. Paul mammoths have a 1.3‰ higher mean $\delta^{13}C_{COLL}$ value while their $\delta^{15}N_{COLL}$ values are largely overlapping. Increasing aridity inferred from several proxies was implicated as the cause of a

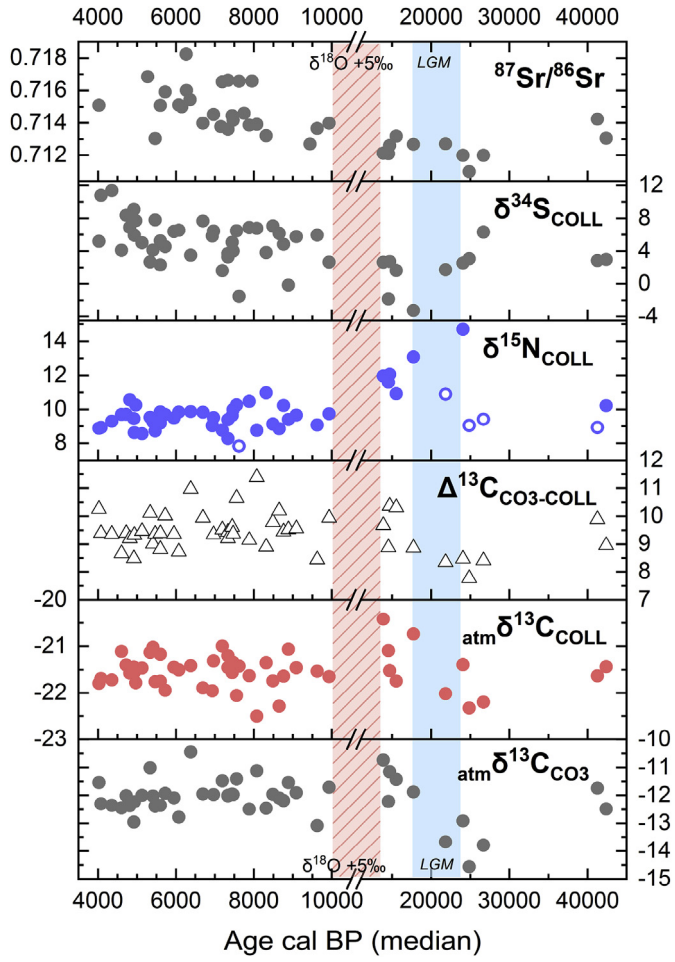

Fig. 5. Isotope values of strontium in bioapatite ($^{87}Sr/^{86}Sr$; Arppe et al., 2009), sulfur ($\delta^{34}S$), nitrogen ($\delta^{15}N$) and carbon ($_{atm}\delta^{13}C_{COLL}$) in collagen, carbon in structural carbonate ($_{atm}\delta^{13}C_{CO3}$) and the difference of carbonate and collagen $\delta^{13}C$ values ($\Delta^{13}C_{CO3\text{-}COLL}$) in mammoth teeth and bones from Wrangel Island. Plots for $_{atm}\delta^{13}C_{Coll}$ and $\delta^{15}N_{COLL}$ include one sample from Szpak et al. (2010). $\delta^{13}C$ values for samples dated to <12 ka have been adjusted a +0.5 due to changes in atmospheric CO_2 (see 2.4). $\delta^{15}N_{COLL}$ data are shown without the "bone-equivalent" adjustment (see 4.1.1), but bone specimens are indicated with white symbol interior. Vertical shadings indicate the Last Glacial Maximum, and the time interval over which Wrangel mammoth enamel $\delta^{18}O$ values show an increase of ~5‰ (Karhu et al., 1998). Note the break and change of scale in the temporal axis to facilitate better separation of Holocene samples.

suggestive rising temporal trend in St. Paul mammoth $\delta^{15}N_{COLL}$ values by Graham et al. (2016) in a study of the causes of extirpation of the island's mammoth population. The $\delta^{13}C_{COLL}$ data were not discussed. As a whole, the high $\delta^{13}C_{COLL}$ levels are consistent with dietary $\delta^{13}C$ values at the level of grasses and sedges growing on dry and coastal/saline sites in present-day Alaska and Yukon territory (Wooller et al., 2007), taking into account an approximate baseline $\delta^{13}C$–CO_2 difference of ~1.5‰ between pre- and post-anthropogenic Holocene (e.g. Leuenberger, 2007). Thus, in addition to aridity, soil salinity as input from sea spray and/or elevations in subsoil saline water table (i.e. sea level) may thus well have influenced the increased $\delta^{13}C_{COLL}$ and $\delta^{15}N_{COLL}$ values in mammoths via its effect on soils and plants as an additional factor (Brugnoli and Lauteri, 1991; Heaton, 1987; Kohn, 2010). However, we note that there is no increasing temporal trend, not even a suggestive one, in St. Paul mammoth $\delta^{13}C_{COLL}$ values. This argues somewhat against a trend of increasing aridity of the system as the sole cause of the higher $\delta^{15}N_{COLL}$ values of mid-Holocene mammoths, unless other factors explaining the random behavior of the $\delta^{13}C_{COLL}$ values come to light. Both very high and low $\delta^{13}C_{COLL}$ values are observed from the start, and relatively low values are observed prior to extinction, contrary to the expected pattern of $\delta^{13}C_{COLL}$ values increasing with assumed increasing aridity. Additional scenarios, such as a cumulative impact of animal activity on the habitat, considered by Graham et al. (2016) as a deleterious influence on freshwater quality but not on forage, could have contributed to the rising $\delta^{15}N_{COLL}$ values. For example, a significant impact of large ungulates on the N cycling of grassland was reported for Yellowstone National Park, with dung and urine input to the soils enhancing ammonia volatilization and denitrification leading to ^{15}N enrichment of soils and plants, and overall N losses from the system (Frank and Evans, 1997).

An additionally conspicuous feature of the St. Paul mammoth $\delta^{13}C_{COLL}$ and $\delta^{15}N_{COLL}$ data is the high level of scatter compared to Wrangel Island (Fig. 2). In spite of the diminutive size of St. Paul Island, ca. 7 km × 16 km, its' mammoths display very heterogeneous isotopic values. Their $\delta^{13}C_{COLL}$ and $\delta^{15}N_{COLL}$ values show ranges of 1.8‰ and 4.8‰ respectively. Holocene mammoths on Wrangel Island show narrower corresponding ranges at 1.5‰ and 3.1‰, despite the much larger island size (ca. 65 km × 135 km) with known significant contrasts in meteorological variables, relief, soils and habitats in different parts of the island (Directorate of Wrangel Island Reserve, 2004). At first glance the high variability of the isotope values of St. Paul mammoths, especially $\delta^{15}N_{COLL}$, seems counterintuitive in such a constrained habitat, but upon further consideration not. Due to the very restricted size of the island, the chances of the mammoths to respond to habitat deterioration by shifting foraging areas would have been very limited. It is likely that the highly variable $\delta^{15}N_{COLL}$ levels are illustrative of a population in an ecological cul-de-sac, much at the mercy of environmental perturbations. Thus, they may actually serve as a potential indicator of a population with a reduced capacity to maintain their ecological niche. Hopefully new mammoth materials will be discovered on St. Paul Island and their analysis will facilitate a more rigorous examination of temporal trends. Furthermore, analyses of S and Sr isotopes would shed interesting light on the intensity of marine influence and landscape use of the animals and their possible role on the observed $\delta^{15}N_{COLL}$ and $\delta^{13}C_{COLL}$ values.

4.2. $\delta^{34}S$ values

The $\delta^{34}S_{COLL}$ values of terrestrial herbivores can serve as indicators of mobility and habitat use (Drucker et al., 2018, 2012; Wißing et al., 2019, 2015) based on the premise that they are controlled by location-specific factors related to the $\delta^{34}S$ values of soils, stemming from local geological formations, sea spray and atmospheric input (see review by Nehlich, 2015). Notwithstanding the two specimens showing negative $\delta^{34}S_{COLL}$ values leading to the apparently low pre-isolation mean $\delta^{34}S_{COLL}$ value in Table 1, the $\delta^{34}S_{COLL}$ values of Wrangel mammoths dating to the time before island isolation are comparable to the $\delta^{34}S_{COLL}$ values of the Bykovsky peninsula mammoths (Fig. 5, Suppl. Fig. 2). Together they appear to define a similar baseline range of bioavailable sulfur for the late Pleistocene in these parts of northern Siberia, with isotopic compositions from ca. +2 to +6‰. Mammoth $\delta^{34}S_{COLL}$ values postdating the isolation of Wrangel Island, in contrast, are higher ranging up to +11.4‰ and indicate increased incorporation of sulfur from a new source with a relatively high $\delta^{34}S$ value. A likely scenario contributing to the elevated $\delta^{34}S_{COLL}$ levels in the island population relates to the rise of sea level at the end of the Pleistocene epoch, resulting in increased input of aerosols carrying the high $\delta^{34}S$ signature of marine sulphates at ca. +20‰ on terrestrial soils and plants, a phenomenon known as the sea-spray effect (Böttcher et al., 2007). An additional potential source of isotopically

distinct sulfur comes from the Proterozoic and Paleozoic bedrock formations of the central mountains of Wrangel Island, discussed further below.

4.3. Wrangel Island mammoths – synthesis

The currently available isotopic data for Wrangel Island mammoths are shown in their temporal context in Fig. 5. Insight into the climatic backdrop for the Wrangel Island mammoths is additionally available from a brief account of the $\delta^{18}O$ values of their tooth enamel (Karhu et al., 1998; Saarnisto and Karhu, 2004) showing a ~5‰ increase ($\delta^{18}O_{CO3}$ from +14 to +19‰, $\delta^{18}O_{PO4}$ from +5 to +10‰) across the Pleistocene-Holocene transition at 14–10 ka. These can be compared to the results of climate simulation by Bryson et al. (2010), employing a high-resolution Macrophysical Climate Model downscaling global predictions of past climatic regimes based on volcanism, orbital forcing parameters and other physical factors (Bryson and McEnaney DeWall, 2007). Consistent with the mammoth oxygen isotope data, Bryson et al. (2010) modeled 8 °C and 5 °C increases in local July and January temperatures, respectively, over the same time interval. The higher July and lower January temperature increase relates to the different stage of Earth's orbital precession in the early Holocene, resulting in greatly enhanced seasonal contrasts in terms of solar energy for Wrangel Island, i.e. warmer summers and colder winters than today. The post-glacial/early Holocene summer thermal optimum is also reflected in paleobotanical records from the island (Lozhkin et al., 2001; Vartanyan, 1997). The Bryson et al. (2010) model predicted steadily increasing winter temperatures and a decline in summer temperature after a warm early Holocene 10–5.5 ka, which was also characterized by markedly stable dry conditions. Thereafter decreased summer temperatures and increased precipitation, mostly as snow, was interpreted to have led to the decline and ultimately termination of grass production and as a consequence, the mammoth population, at 4 ka (Bryson et al., 2010). In strong contrast to this model based prediction, the stability of the $\delta^{13}C_{COLL}$, $\delta^{13}C_{CO3}$, $\delta^{15}N_{COLL}$ and $\Delta^{13}C_{COLL\text{-}CO3}$ values does not support such a significant change of forage characteristics for Wrangel mammoths younger than 5.5 ka compared to the older ones, since such a change would have impacted on the forage strategy of the mammoths and changed their isotopic values. This discrepancy can have different sources. Either the modeled temperatures are not reflecting the actual temperatures on Wrangel Island, or they are basically correct but additional factors prevented the productivity from decreasing, such as the fertilizing role of the mammoths themselves. Indeed, the productivity of tundra ecosystems is more limited by nutrient depletion than by temperatures (e.g. Jonasson et al., 1999). Additionally the prediction for grass productivity as a function of seasonal temperatures was based on an analogy with Iceland (Bryson et al., 2010), where the environmental conditions are clearly different from those on Wrangel Island. Today on Wrangel Island, grassland continues to grow with July temperatures at 1–4 °C thanks to high animal nitrogen input (Zimov et al., 2012). It is therefore conceivable that the occurrence of mammoths and other large herbivores on Wrangel Island buffered the effects of the modeled climatic fluctuations during the Holocene and allowed the forage supply to be maintained.

The strontium and sulfur isotope data allow us a glimpse into the evolution of landscape use by the mammoths of Wrangel Island. Reflecting bioavailable Sr largely derived from geological substrate, the elevated mean $^{87}Sr/^{86}Sr$ level of the post-isolation Wrangel Island mammoths was interpreted as an influence of radiogenic Sr derived from Neoproterozoic rocks in the central mountains (Arppe et al., 2009). The increased $^{87}Sr/^{86}Sr$ ratios after the first 2000 years of isolation were found to match the temporal pattern of a major reduction of island area taking place by 8 ka (Arppe et al., 2009; Manley, 2002). It is interesting to compare these data to the landscape use proxy obtained in this study, the collagen $\delta^{34}S_{COLL}$ values. Both display rising trends in Fig. 5. The mean $\delta^{34}S_{COLL}$ levels of the post-isolation samples are significantly higher than those predating the isolation. Furthermore, the mean $\delta^{34}S_{COLL}$ value of samples dating to the last 1000 years prior to extinction (5–4 ka; +7.7‰ ± 2.5) as compared to the preceding 5000 years (+4.7‰ ± 2.2) was yet significantly higher. As discussed earlier, a possible source for the rising $\delta^{34}S_{COLL}$ after island isolation is provided by marine sulphate with $\delta^{34}S$ values at ~+20‰ (Rees et al., 1978). However, the island area remained constant after 8 ka, so the further increase in $\delta^{34}S_{COLL}$ over the last millennia should not be related to ever increasing marine influence. This is also supported by the fact that the increasing $\delta^{34}S_{COLL}$ values are not accompanied by decreasing $^{87}Sr/^{86}Sr$ values, the expected signal for marine influence. It is also not plausible that the mammoths shifted to consuming more plants from the immediate coastal zone, as this would have also affected their $\delta^{13}C$ and $\delta^{15}N$ values accordingly. Comparably to Sr, another source of sulfur to the soil sulphate pool sampled by plants is the local bedrock. For example, the Early Carboniferous strata of the central mountains are known to contain extensive beds of gypsum (Lavrushin and Gruzdev, 2012), expected to have relatively high $\delta^{34}S$ values (Nehlich, 2015). Increased chemical weathering of the central mountain geological formations as a result of the modeled increase in precipitation at 5.5–4 ka (Bryson et al., 2010) could account for the increasing $\delta^{34}S_{COLL}$ values towards the end of the mammoth record.

Although the isotope records of Wrangel Island mammoths do not indicate a loss of the typical, optimal mammoth habitat/feeding niche as reported by Drucker et al. (2018) for other mammoth populations shortly before their extirpation, and testify against long-term deterioration of plant growth hypothesized by Bryson et al. (2010), there still might be food and drinking water related, hitherto unexplored, environmental factors that might have contributed to their extinction. Wrangel Island has more than 1400 rivers and streams, which likely served as sources of drinking water to the animals. A recent survey of the chemical composition of the island's extensive fluvial networks discovered levels of overall mineralization, measured as the total dissolved solids (TDS), that were an order of magnitude higher than typical small rivers of the Arctic region (0.3–2 g/l; Lavrushin and Gruzdev, 2012). Over the 5-year sampling period, some rivers intermittently showed white, red and bluish coloring, very high TDS loads (6.5–23 g/l) coupled with very low pH values at 2.4–4.6 and an enrichment of heavy metals and other toxic elements (e.g. Cd, Pb, U, Th). The levels of some elements, some considered toxic, exceeded levels that are considered recommendable over the long-term (S, Mg) or safe (Cd, Al, Mn) for livestock drinking water by the FAO (Ayers and Westcot, 1985). The origin of these qualities were traced back to the leaching of gypsum-bearing rocks at the source area of most rivers, and the weathering of sulfide, base metal, copper and antimony ores in the central mountains (Lavrushin and Gruzdev, 2012). High TDS loads seem to be a common feature of Wrangel Island rivers, but it is unclear under which circumstances potentially harmful amounts of micro and macro elements are leached out. Some of the highest anomalies were recorded after an especially warm summer that had resulted in enhanced thawing of permafrost and erosion and alteration of the underlying rocks (Lavrushin and Gruzdev, 2012). Despite the generally arid and cold climate, a peculiar elevated thermal regime characterizes the central intermontane hollows where frequently occurring foehn type winds, i.e. dry and warm winds occurring on the lee-side of mountains, may cause sharp temperature increases (Directorate of Wrangel Island Reserve, 2004). As proposed above for the $\delta^{34}S_{COLL}$ record, perhaps

intensified weathering at 5.5–4 ka resulted in adverse effects for water quality, including more frequent releases of harmful substances in the rivers. Geochemical changes linked to the impact of Holocene climate change on soil chemistry has been hypothesized as a possible cause of mammoth and other megafauna extinction in northern Eurasia, seemingly supported by an increase of bone growth deficiencies in the latest Pleistocene (Leshchinskiy, 2015). Decreased freshwater quality and availability evidently contributed to the extinction of the Holocene mammoth population on St. Paul Island (Graham et al., 2016; Wang et al., 2018). It now seems possible that also Wrangel Island mammoths could have faced issues of suboptimal water quality contributing towards reduced fitness of the population, if not direct toxic effects.

While the isotope data do not support a long-term decline in food resources, short-term dietary crises would not be registered due to the slow integrative formation and remodeling of skeletal tissues and the bulk sampling method employed here. Winter is and was the nemesis of many animals in the high Arctic. Food is scarcer, of lower quality and harder to access, and the low temperatures impart higher thermoregulatory costs to the animal. Analyzing dentine layers in tusks El Adli et al. (2017) report the life histories of five woolly mammoths, two Pleistocene individuals from Chukotka and three Holocene animals from Wrangel Island, and conclude that all of them died in the winter. During winter 2003, an extreme rain-on-snow event on Banks Island, high Arctic Canada, led to pervasive icing of the snowpack, preventing access to food. 20,000 musk-oxen starved to death (Putkonen et al., 2009). On Wrangel Island, reindeer deaths of hundreds to thousands of individuals have occurred after winter icing episodes. The events can be catastrophic to the population and appear to occur fairly often (Berger et al., 2018; Mizin et al., 2018). Extreme icing events are rare and their current probability is likely elevated due to climate warming (Berger et al., 2018), but it is conceivable such events could have occurred also earlier in the Holocene, and that their probability increased with the increased precipitation at 5.5–4 ka and rising winter temperatures modeled for Wrangel Island (Bryson et al., 2010). One might hypothesize, that an already weakened and decreased (Palkopoulou et al., 2015; Rogers and Slatkin, 2017) population, one that has perhaps adapted towards less resilience against long-term starvation (cf. higher $\delta^{13}C_{CO3}$ values compared to full-glacial Siberian mammoths), might succumb to an extreme icing event.

The inferred stability in mammoth dietary ecology until the end of their presence on Wrangel Island, despite climate change and decreasing genetic diversity, suggests that possible scenarios for the final extinction of Wrangel island mammoths some 4000 years ago might involve unusual short-term crises or agents simply not registered in the commonly analysed bulk sample isotope compositions. An additional possible scenario that cannot be ruled out nor tested with the available evidence is human involvement. Despite the currently standing temporal mismatch of records for the latest presence of mammoths and earliest presence of humans on the island, there were several prehistoric cultures present in Chukotka contemporaneous with the Wrangel Island mammoths (e.g. Kuzmin, 2000; Slobodin, 2012). The idea of prehistoric hunters visiting the island and encountering mammoths cannot be excluded on simple grounds of absence of archaeological evidence, as probabilities of finding such evidence is low due to demographic and taphonomic biases (Surovell and Grund, 2012). Some insight into the role of humans and other short-term or catastrophic factors in the demise of the Wrangel Island mammoths may be provided by detailed studies of tusk growth increments for signs of predation pressure (Fisher, 2009) and by means of isotopic analyses of microsamples from the very last months and weeks of life.

5. Conclusions

The multi-isotopic evidence measured on directly dated Wrangel Island mammoths indicates that they did not face extinction due to a gradual deterioration of forage availability and quality, and supports the idea that this relict population could maintain a typical mammoth ecology despite climate change and decreasing genetic diversity. Despite providing evidence against a gradual decline in dietary wellbeing, it might be possible that the already weakened population fell victim to a sudden starvation event, such as an extreme icing event preventing access to food.

In terms of isotopic ecology, especially the dietary protein inferred from collagen $\delta^{13}C$ and $\delta^{15}N$ values, the Holocene Wrangel Island mammoths were very similar to their northern Beringian forebears. The available bioapatite carbonate $\delta^{13}C$ records suggest, however, that they were distinct from the Pleistocene mainland Siberian mammoths in terms of their energy economy. This is possibly related to more use of reserve fats during harsher winter conditions or a difference in digestive processing for Siberian mammoths.

Sulfur and strontium isotope values reflect the increased influence of the sea spray effect and the special characteristics of local bedrock for the island population. The possibly increased effects of bedrock derived harmful macro and microelements ingested by the mammoths via drinking water towards the end of the mammoth record are hinted at by these bedrock-derived isotope proxies. The speculated increased weathering input highlights a previously undiscovered possibility of water quality problems for the mammoth population, related to a very high level of total dissolved solids and apparent intermittent emissions of toxic elements into the fluvial systems from the mineralizations of the central mountains of Wrangel Island.

Our study shows that Wrangel Island maintained through the Holocene, and possibly until the present day, environmental conditions suitable for a typical mammoth ecological niche. This is in stark contrast to St. Paul Island, the only other insular Holocene mammoth population documented so far, where the animals apparently were much more susceptible to environmental disruptions due to the limited size of the island, finally leading to the extirpation of the population without human influence. The exact cause of final extinction for the Wrangel Island mammoths remains equivocal, but we suggest it was likely caused by a short-term crisis, possibly linked to climatic anomalies or/and geochemical factors. Furthermore, anthropogenic influence should not be ruled out despite lack of tangible evidence of hunting.

On a methodological level this study demonstrates how multi-isotopic tracking can distinguish different scenarios for mammoth extirpation in different parts of their geographical distribution, from mammoths of mainland Beringia and Wrangel Island that kept their ecological niche until their final regional disappearance, to the detrimental change in ecological niche seen for some low latitude Eurasian sites, and finally, the unique and contrasting isotopic pattern of the insular mammoths of St Paul Island. The variable isotopic patterns for the woolly mammoth in different regions of their distribution area show that the extinction of this emblematic ice age species cannot be attributed to one determining cause, but that following fragmentation of their distribution, each remaining population had a different trajectory where different factors led to the final extirpation of each population. Further isotopic tracking of last members of extinct Pleistocene mammals through their range should help to decipher the complex process of species extinction and maybe provide further insight to help preserve the remaining ones.

Data availability

All data used in this article are provided in the Appendices accompanying this paper.

Acknowledgements

We thank B. Steinhilber, H. Taubald, C. Must and S. Ali for their technical support for the isotopic analysis in Tübingen. Financial support was provided by the DAAD (Deutscher Akademischer Austauschdienst), Germany, project #54751123 and by the Academy of Finland, Finland, grant #SA259548 for traveling and research visits in Helsinki and Tübingen during the realization of this study. Dr. Pavel Grebenyuk is sincerely thanked for discussions of prehistoric human presence in the region. Two anonymous reviewers are thanked for taking the time to review the paper and give constructive comments.

Appendices and Supplementary data

Supplementary data (Appendix A, Appendix B and supplementary figures) to this article can be found online at https://doi.org/10.1016/j.quascirev.2019.105884.

References

Ambrose, S.H., 1990. Preparation and characterization of bone and tooth collagen for isotopic analysis. J. Archaeol. Sci. 17, 431–451. https://doi.org/10.1016/0305-4403(90)90007-R.

Ambrose, S.H., DeNiro, M.J., 1986. The isotopic ecology of East African mammals. Oecologia 69, 395–406. https://doi.org/10.1007/BF00377062.

Ambrose, S.H., Norr, L., 1993. Experimental evidence for the relationship of the carbon isotope ratios of whole diet and dietary protein to those of bone collagen and carbonate. In: Prehistoric Human Bone. Springer Berlin Heidelberg, Berlin, Heidelberg, pp. 1–37. https://doi.org/10.1007/978-3-662-02894-0_1.

Amrhein, V., Valentin, A., Sander, G., Blake, M., 2019. Retire statistical significance. Nature 567, 305–307. https://doi.org/10.1038/d41586-019-00857-9.

Arppe, L., Karhu, J.A., Vartanyan, S.L., 2009. Bioapatite $^{87}Sr/^{86}Sr$ of the last woolly mammoths - implications for the isolation of Wrangel Island. Geology 37, 347–350. https://doi.org/10.1130/G25467A.1.

Ayers, R.S., Westcot, D.W., 1985. Water Quality for Agriculture. Food and Agriculture Organization of the United Nations, Rome. https://doi.org/10.1016/S1040-6182(01)00083-0.

Barbieri, M., Kuznetsova, T.V., Nikolaev, V.I., Palombo, M.R., 2008. Strontium isotopic composition in late Pleistocene mammal bones from the Yakutian region (North-Eastern Siberia). Quat. Int. 179, 72–78. https://doi.org/10.1016/j.quaint.2007.08.014.

Barnes, I., Shapiro, B., Lister, A., Kuznetsova, T., Sher, A., Guthrie, D., Thomas, M.G., 2007. Genetic structure and extinction of the woolly mammoth, *Mammuthus primigenius*. Curr. Biol. 17, 1072–1075. https://doi.org/10.1016/J.CUB.2007.05.035.

Bartlett, L.J., Williams, D.R., Prescott, G.W., Balmford, A., Green, R.E., Eriksson, A., Valdes, P.J., Singarayer, J.S., Manica, A., 2016. Robustness despite uncertainty: regional climate data reveal the dominant role of humans in explaining global extinctions of Late Quaternary megafauna. Ecography (Cop.). 39, 152–161. https://doi.org/10.1111/ecog.01566.

Berger, J., Hartway, C., Gruzdev, A., Johnson, M., 2018. Climate degradation and extreme icing events constrain life in cold-adapted mammals. Sci. Rep. 8, 1156. https://doi.org/10.1038/s41598-018-19416-9.

Bocherens, H., 2003. Isotopic biogeochemistry and the paleoecology of the mammoth steppe fauna. Deinsea 9 (57–76) [ISSN 0923-9308].

Bocherens, H., Billiou, D., Patou-Mathis, M., Bonjean, D., Otte, M., Mariotti, A., 1997. Paleobiological implications of the isotopic signatures (^{13}C,^{15}N) of fossil mammal collagen in scladina cave (sclayn, Belgium). Quat. Res. 48, 370–380. https://doi.org/10.1006/qres.1997.1927.

Bocherens, H., Drucker, D.G., Germonpré, M., Lázničková-Galetová, M., Naito, Y.I., Wissing, C., Brůžek, J., Oliva, M., 2015. Reconstruction of the Gravettian food-web at Předmostí I using multi-isotopic tracking (^{13}C, ^{15}N, ^{34}S) of bone collagen. Quat. Int. 359, 211–228. https://doi.org/10.1016/j.quaint.2014.09.044.

Bocherens, H., Drucker, D.G., Taubald, H., 2011. Preservation of bone collagen sulphur isotopic compositions in an early Holocene river-bank archaeological site. Palaeogeogr. Palaeoclimatol. Palaeoecol. 310, 32–38. https://doi.org/10.1016/j.palaeo.2011.05.016.

Bocherens, H., Fizet, M., Mariotti, A., Gangloff, R.A., Burns, J.A., 1994. Contribution of isotopic biogeochemistry (^{13}C, ^{15}N, ^{18}O) to the paleoecology of mammoths (*Mammuthus primigenius*). Hist. Biol. 7, 187–202. https://doi.org/10.1080/10292389409380453.

Bocherens, H., Pacaud, G., Lazarev, P.A., Mariotti, A., 1996. Stable isotope abundances (^{13}C, ^{15}N) in collagen and soft tissues from Pleistocene mammals from Yakutia: implications for the palaeobiology of the Mammoth Steppe. Palaeogeogr. Palaeoclimatol. Palaeoecol. 126, 31–44. https://doi.org/10.1016/S0031-0182(96)00068-5.

Böttcher, M.E., Brumsack, H.-J., Dürselen, C.-D., 2007. The isotopic composition of modern seawater sulfate: I. Coastal waters with special regard to the North Sea. J. Mar. Syst. 67, 73–82. https://doi.org/10.1016/J.JMARSYS.2006.09.006.

Breecker, D.O., 2017. Atmospheric pCO_2 control on speleothem stable carbon isotope compositions. Earth Planet. Sci. Lett. 458, 58–68. https://doi.org/10.1016/J.EPSL.2016.10.042.

Bronshtein, M.M., Dneprovsky, K.A., Savinetsky, A.B., 2016. Ancient eskimo cultures of Chukotka. In: Friesen, M., Mason, O. (Eds.), Oxford Handbook of the Prehistoric Arctic. Oxford University Press, New York, pp. 489–511. https://doi.org/10.1093/oxfordhb/9780199766956.013.53.

Brugnoli, E., Lauteri, M., 1991. Effects of salinity on stomatal conductance, photosynthetic capacity, and carbon isotope discrimination of salt-tolerant (Gossypium hirsutum L.) and salt-sensitive (Phaseolus vulgaris L.) C3 nonhalophytes. Plant Physiol. 95, 628–635. https://doi.org/10.1104/PP.95.2.628.

Bryson, R.A., McEnaney DeWall, K. (Eds.), 2007. A Paleoclimatology workbook: high resolution, site-specific, macrophysical climate modeling. The Mammoth Site of Hot Springs, South Dakota, p. 288.

Bryson, R.A., Agenbroad, L.D., McEnaney DeWall, K., 2010. Paleoclimate modeling and paleoenvironmental interpretations for three instances of island dwelling mammoths. Quat. Int. 217, 6–9. https://doi.org/10.1016/j.quaint.2009.09.028.

Clementz, M.T., Fox-Dobbs, K., Wheatley, P.V., Koch, P.L., Doak, D.F., 2009. Revisiting old bones: coupled carbon isotope analysis of bioapatite and collagen as an ecological and palaeoecological tool. Geol. J. 44, 605–620. https://doi.org/10.1002/gj.1173.

Codron, D., Clauss, M., Codron, J., Tütken, T., 2018. Within trophic level shifts in collagen-carbonate stable carbon isotope spacing are propagated by diet and digestive physiology in large mammal herbivores. Ecol. Evol. 8, 3983–3995. https://doi.org/10.1002/ece3.3786.

Coplen, T.B., Brand, W.A., Gehre, M., Gröning, M., Meijer, H.A.J., Toman, B., Verkouteren, R.M., 2006. New guidelines for $\delta^{13}C$ measurements. Anal. Chem. 78, 2439–2441. https://doi.org/10.1021/ac052027c.

Craine, J., Elmore, A.J., Aidar, M.P.M., Bustamante, M., Dawson, T.E., Hobbie, E., Kahmen, A., Mack, M.C., Mclauchlan, K.K., Michelsen, A., Nardoto, G.B., Pardo, L.H., 2009. Global patterns of foliar nitrogen isotopes and their relationships. New Phytol. 183, 980–992. https://doi.org/10.1111/j.1469-8137.2009.02917.x.

Debruyne, R., Chu, G., King, C.E., Bos, K., Kuch, M., Schwarz, C., Szpak, P., Gröcke, D.R., Matheus, P., Zazula, G., Guthrie, D., Froese, D., Buigues, B., de Marliave, C., Flemming, C., Poinar, D., Fisher, D., Southon, J., Tikhonov, A.N., MacPhee, R.D.E., Poinar, H.N., 2008. Out of America: ancient DNA evidence for a new world origin of late quaternary woolly mammoths. Curr. Biol. 18, 1320–1326. https://doi.org/10.1016/j.cub.2008.07.061.

DeNiro, M.J., 1985. Postmortem preservation and alteration of in vivo bone collagen isotope ratios in relation to palaeodietary reconstruction. Nature 317, 806–809.

DeNiro, M.J., Epstein, S., 1981. Influence of diet on the distribution of nitrogen isotopes in animals. Geochim. Cosmochim. Acta 45, 341–351. https://doi.org/10.1016/0016-7037(78)90199-0.

DeNiro, M.J., Epstein, S., 1978. Influence of diet on the distribution of carbon isotopes in animals. Geochim. Cosmochim. Acta 42, 495–506.

DeNiro, M.J., Weiner, S., 1988. Chemical, enzymatic and spectroscopic characterization of "collagen" and other organic fractions from prehistoric bones. Geochim. Cosmochim. Acta 52, 2197–2206. https://doi.org/10.1016/0016-7037(88)90122-6.

Directorate of Wrangel Island Reserve, 2004. Natural System of Wrangel Island Reserve for Inscription into the World Cultural and Natural Heritage List of UNESCO [WWW Document].

Doi, H., Akamatsu, F., González, A.L., 2017. Starvation effects on nitrogen and carbon stable isotopes of animals: an insight from meta-analysis of fasting experiments. R. Soc. Open Sci. 4, 170633. https://doi.org/10.1098/rsos.170633.

Drucker, D.G., Bocherens, H., Péan, S., 2014. Isotopes stables (^{13}C, ^{15}N) du collagène des mammouths de Mezhyrich (Epigravettien, Ukraine) : implications paléoécologiques. Anthropologie 118, 504–517. https://doi.org/10.1016/j.anthro.2014.04.001.

Drucker, D.G., Bridault, A., Cupillard, C., 2012. Environmental context of the Magdalenian settlement in the Jura Mountains using stable isotope tracking (^{13}C, ^{15}N, ^{34}S) of bone collagen from reindeer (*Rangifer tarandus*). Quat. Int. 272–273, 322–332. https://doi.org/10.1016/J.QUAINT.2012.05.040.

Drucker, D.G., Bridault, A., Hobson, K.A., Szuma, E., Bocherens, H., 2008. Can carbon-13 in large herbivores reflect the canopy effect in temperate and boreal ecosystems? Evidence from modern and ancient ungulates. Palaeogeogr. Palaeoclimatol. Palaeoecol. 266, 69–82. https://doi.org/10.1016/J.PALAEO.2008.03.020.

Drucker, D.G., Stevens, R.E., Germonpré, M., Sablin, M.V., Péan, S., Bocherens, H., 2018. Collagen stable isotopes provide insights into the end of the mammoth steppe in the central East European plains during the Epigravettian. Quat. Res. 90, 457–469. https://doi.org/10.1017/qua.2018.40.

Drucker, D.G., Vercoutère, C., Chiotti, L., Nespoulet, R., Crépin, L., Conard, N.J., Münzel, S.C., Higham, T., van der Plicht, J., Láznicková-Galetová, M., Bocherens, H., 2015. Tracking possible decline of woolly mammoth during the

Gravettian in Dordogne (France) and the Ach Valley (Germany) using multi-isotope tracking (^{13}C, ^{14}C, ^{15}N, ^{34}S, ^{18}O). Quat. Int. 359–360, 304–317. https://doi.org/10.1016/j.quaint.2014.11.028.

Eggleston, S., Schmitt, J., Bereiter, B., Schneider, R., Fischer, H., 2016. Evolution of the stable carbon isotope composition of atmospheric CO_2 over the last glacial cycle. Paleoceanography 31, 434–452. https://doi.org/10.1002/2015PA002874.

El Adli, J.J., Fisher, D.C., Vartanyan, S.L., Tikhonov, A.N., 2017. Final years of life and seasons of death of woolly mammoths from Wrangel Island and mainland Chukotka, Russian Federation. Quat. Int. 445, 135–145. https://doi.org/10.1016/j.quaint.2016.07.017.

Fellows Yates, J.A., Drucker, D.G., Reiter, E., Heumos, S., Welker, F., Münzel, S.C., Wojtal, P., Lázničková-Galetová, M., Conard, N.J., Herbig, A., Bocherens, H., Krause, J., 2017. Central European woolly mammoth population dynamics: insights from late Pleistocene mitochondrial genomes. Sci. Rep. 7, 17714. https://doi.org/10.1038/s41598-017-17723-1.

Fisher, D.C., 2009. Paleobiology and Extinction of Proboscideans in the Great Lakes Region of North America. Springer, Dordrecht, pp. 55–75. https://doi.org/10.1007/978-1-4020-8793-6_4.

Fox-Dobbs, K., Leonard, J.A., Koch, P.L., 2008. Pleistocene megafauna from eastern Beringia: paleoecological and paleoenvironmental interpretations of stable carbon and nitrogen isotope and radiocarbon records. Palaeogeogr. Palaeoclimatol. Palaeoecol. 261, 30–46. https://doi.org/10.1016/J.PALAEO.2007.12.011.

Frank, D.A., Evans, R.D., 1997. Effects of native grazers on grassland N cycling in Yellowstone national Park. Ecology 78, 2238–2248. https://doi.org/10.1890/0012-9658(1997)078[2238:EONGOG]2.0.CO;2.

Gerasimov, D.V., Giria, E.Y., Pitul'ko, V.V., Tikhonov, A.N., 2006. New materials for the interpretation of the Chertov Ovrag site on Wrangel island. In: Dumond, D.E., Bland, R.L. (Eds.), Archaeology in Northeast Asia: on the Pathway to Bering Strait. Museum of Natural and Cultural History, and Department of Anthropology, University of Oregon, pp. 203–206.

Graham, R.W., Belmecheri, S., Choy, K., Culleton, B.J., Davies, L.J., Froese, D., Heintzman, P.D., Hritz, C., Kapp, J.D., Newsom, L.A., Rawcliffe, R., Saulnier-Talbot, É., Shapiro, B., Wang, Y., Williams, J.W., Wooller, M.J., 2016. Timing and causes of mid-Holocene mammoth extinction on St. Paul Island, Alaska. Proc. Natl. Acad. Sci. 113, 201604903. https://doi.org/10.1073/pnas.1604903113.

Grigoriev, S.E., Fisher, D.C., Obadă, T., Shirley, E.A., Rountrey, A.N., Savvinov, G.N., Garmaeva, D.K., Novgorodov, G.P., Cheprasov, M.Y., Vasilev, S.E., Goncharov, A.E., Masharskiy, A., Egorova, V.E., Petrova, P.P., Egorova, E.E., Akhremenko, Y.A., van der Plicht, J., Galanin, A.A., Fedorov, S.E., Ivanov, E.V., Tikhonov, A.N., 2017. A woolly mammoth (*Mammuthus primigenius*) carcass from maly Lyakhovsky island (new siberian islands, Russian Federation). Quat. Int. 445, 89–103. https://doi.org/10.1016/j.quaint.2017.01.007.

Guthrie, R.D., 2006. New carbon dates link climatic change with human colonization and Pleistocene extinctions. Nature 441, 207–209. https://doi.org/10.1038/nature04604.

Guthrie, R.D., 2004. Radiocarbon evidence of mid-Holocene mammoths stranded on an Alaskan Bering Sea island. Nature 429, 746–749. https://doi.org/10.1038/nature02612.

Haesaerts, P., Péan, S., Valladas, H., Damblon, F., Nuzhnyi, D., 2015. Contribution à la stratigraphie du site paléolithique de Mezhyrich (Ukraine). Anthropologie 119, 364–393. https://doi.org/10.1016/j.anthro.2015.07.002.

Hare, V.J., Loftus, E., Jeffrey, A., Bronk Ramsey, C., 2018. Atmospheric CO_2 effect on stable carbon isotope composition of terrestrial fossil archives. Nat. Commun. 9, 252. https://doi.org/10.1038/s41467-017-02691-x.

Hatch, K.A., 2012. The use and application of stable isotope analysis to the study of starvation, fasting, and nutritional stress in animals. In: McCue, M.D. (Ed.), Comparative Physiology of Fasting, Starvation, and Food Limitation. Springer Berlin Heidelberg, Berlin, Heidelberg, pp. 337–364. https://doi.org/10.1007/978-3-642-29056-5_20.

Hatté, C., Fontugne, M., Rousseau, D.-D., Antoine, P., Zöller, L., Laborde, N.T., Bentaleb, I., 1998. $\delta^{13}C$ variations of loess organic matter as a record of the vegetation response to climatic changes during the Weichselian. Geology 26, 583. https://doi.org/10.1130/0091-7613(1998)026%3c0583:CVOLOM%3e2.3.CO;2.

Heaton, T.H.E., 1987. The $^{15}N/^{14}N$ ratios of plants in South Africa and Namibia: relationship to climate and coastal/saline environments. Oecologia 74, 236–246. https://doi.org/10.1007/BF00379365.

Hedges, R.E.M., 2003. On bone collagen-apatite-carbonate isotopic relationships. Int. J. Osteoarchaeol. 13, 66–79. https://doi.org/10.1002/oa.660.

Holmes, C.E., 2011. The beringian and transitional periods in Alaska: technology of the East beringian tradition as viewed from swan point. In: Goebel, T.D., Buvit, I. (Eds.), From the Yenisei to the Yukon: Interpreting Lithic Assemblage Variability in Late Pleistocene/Early Holocene Beringia. Texas A&M Press, College Station., pp. 179–191

Iacumin, P., Davanzo, S., Nikolaev, V., 2005. Short-term climatic changes recorded by mammoth hair in the Arctic environment. Palaeogeogr. Palaeoclimatol. Palaeoecol. 218, 317–324. https://doi.org/10.1016/j.palaeo.2004.12.021.

Iacumin, P., Di Matteo, A., Nikolaev, V., Kuznetsova, T.V., 2010. Climate information from C, N and O stable isotope analyses of mammoth bones from northern Siberia. Quat. Int. 212, 206–212. https://doi.org/10.1016/j.quaint.2009.10.009.

Iacumin, P., Nikolaev, V., Ramigni, M., 2000. C and N stable isotope measurements on Eurasian fossil mammals, 40 000 to 10 000 years BP: herbivore physiologies and palaeoenvironmental reconstruction. Palaeogeogr. Palaeoclimatol. Palaeoecol. 163, 33–47. https://doi.org/10.1016/S0031-0182(00)00141-3.

Jim, S., Ambrose, S.H., Evershed, R.P., 2004. Stable carbon isotopic evidence for differences in the dietary origin of bone cholesterol, collagen and apatite: implications for their use in palaeodietary reconstruction. Geochim. Cosmochim. Acta 68, 61–72. https://doi.org/10.1016/S0016-7037(03)00216-3.

Jonasson, S., Michelsen, A., Schmidt, I.K., Nielsen, E.V., 1999. Responses in microbes and plants to changed temperature, nutrient, and light regimes in the Arctic. Ecology 80, 1828–1843. https://doi.org/10.1890/0012-9658(1999)080[1828:RIMAPT]2.0.CO;2.

Karhu, J.A., Possnert, G., Saarnisto, M., Vartanyan, S.L., 1998. Paleoclimatic change at the Pleistocene-Holocene boundary, Wrangel Island, eastern Siberia: evidence from oxygen isotopes in mammoth teeth. In: Eos, Transactions. American Geophysical Union, p. F492.

Kirillova, I.V., Tiunov, A.V., Levchenko, V.A., Chernova, O.F., Yudin, V.G., Bertuch, F., Shidlovskiy, F.K., 2015. On the discovery of a cave lion from the Malyi Anyui river (Chukotka, Russia). Quat. Sci. Rev. 117, 135–151. https://doi.org/10.1016/j.quascirev.2015.03.029.

Kohn, M.J., 2016. Carbon isotope discrimination in C_3 land plants is independent of natural variations in pCO_2. Geochem. Perspect. Lett. 2, 35–43. https://doi.org/10.7185/geochemlet.1604.

Kohn, M.J., 2010. Carbon isotope compositions of terrestrial C_3 plants as indicators of (paleo)ecology and (paleo)climate. Proc. Natl. Acad. Sci. U. S. A. 107, 19691–5. https://doi.org/10.1073/pnas.1004933107.

Kuzmin, Y.V., 2010. Extinction of the woolly mammoth (*Mammuthus primigenius*) and woolly rhinoceros (*Coelodonta antiquitatis*) in Eurasia: review of chronological and environmental issues. Boreas 39, 247–261. https://doi.org/10.1111/j.1502-3885.2009.00122.x.

Kuzmin, Y.V., 2000. Radiocarbon chronology of the stone age cultures on the pacific coast of northeastern Siberia. Arctic Anthropol. 37, 120–131.

Kuzmin, Y.V., Orlova, L.A., 2004. Radiocarbon chronology and environment of woolly mammoth (*Mammuthus primigenius* Blum.) in northern Asia: results and perspectives. Earth Sci. Rev. 68, 133–169. https://doi.org/10.1016/j.earscirev.2004.04.002.

Lanoë, F.B., Holmes, C.E., 2016. Animals as raw material in Beringia: insights from the site of Swan Point CZ4B, Alaska. Am. Antiq. 81, 682–696. https://doi.org/10.1017/S0002731600101039.

Lanoë, F.B., Reuther, J.D., Holmes, C.E., Hodgins, G.W.L., 2017. Human paleoecological integration in subarctic eastern Beringia. Quat. Sci. Rev. 175, 85–96. https://doi.org/10.1016/j.quascirev.2017.10.003.

Lavrushin, V.Y., Gruzdev, A.R., 2012. The salt composition of rivers in Wrangel Island. Lithol. Miner. Resour. 47, 1–17. https://doi.org/10.1134/S0024490211060101.

Leshchinskiy, S., 2015. Enzootic diseases and extinction of mammoths as a reflection of deep geochemical changes in ecosystems of Northern Eurasia. Archaeol. Anthropol. Sci. 7, 297–317. https://doi.org/10.1007/s12520-014-0205-4.

Leuenberger, M., 2007. To what extent can ice core data contribute to the understanding of plant ecological developments of the past? In: Dawson, T.E., Siegwolf, R.T.W. (Eds.), Stable Isotopes as Indicators of Ecological Change, pp. 211–233. Terrestrial Ecology 1.

Lorenzen, E.D., Nogués-Bravo, D., Orlando, L., Weinstock, J., Binladen, J., Marske, K.A., Ugan, A., Borregaard, M.K., Gilbert, M.T.P., Nielsen, R., Ho, S.Y.W., Goebel, T., Graf, K.E., Byers, D., Stenderup, J.T., Rasmussen, M., Campos, P.F., Leonard, J.A., Koepfli, K.-P., Froese, D., Zazula, G., Stafford, T.W., Aaris-Sørensen, K., Batra, P., Haywood, A.M., Singarayer, J.S., Valdes, P.J., Boeskorov, G., Burns, J.A., Davydov, S.P., Haile, J., Jenkins, D.L., Kosintsev, P., Kuznetsova, T., Lai, X., Martin, L.D., McDonald, H.G., Mol, D., Meldgaard, M., Munch, K., Stephan, E., Sablin, M., Sommer, R.S., Sipko, T., Scott, E., Suchard, M.A., Tikhonov, A., Willerslev, R., Wayne, R.K., Cooper, A., Hofreiter, M., Sher, A., Shapiro, B., Rahbek, C., Willerslev, E., 2011. Species-specific responses of Late Quaternary megafauna to climate and humans. Nature 479, 359–364. https://doi.org/10.1038/nature10574.

Lourantou, A., Lavrič, J.V., Köhler, P., Barnola, J.M., Paillard, D., Michel, E., Raynaud, D., Chappellaz, J., 2010. Constraint of the CO_2 rise by new atmospheric carbon isotopic measurements during the last deglaciation. Glob. Biogeochem. Cycles 24, GB2015. https://doi.org/10.1029/2009GB003545.

Lozhkin, A.V., Anderson, P.M., Vartanyan, S.L., Brown, T.A., Belaya, B.V., Kotov, A.N., 2001. Late quaternary paleoenvironments and modern pollen data from Wrangel island (northern Chukotka). Quat. Sci. Rev. 20, 217–233. https://doi.org/10.1016/S0277-3791(00)00121-9.

Lozhkin, A.V., Anderson, P.M., Vazhenina, L.N., 2011. Younger dryas and early Holocene peats from northern far East Russia. Quat. Int. 237, 54–64. https://doi.org/10.1016/j.quaint.2011.01.009.

MacDonald, G.M., Beilman, D.W., Kuzmin, Y.V., Orlova, L.A., Kremenetski, K.V., Shapiro, B., Wayne, R.K., Van Valkenburgh, B., 2012. Pattern of extinction of the woolly mammoth in Beringia. Nat. Commun. 3, 893. https://doi.org/10.1038/ncomms1881.

MacPhee, R.D.E., Tikhonov, A.N., Mol, D., de Marliave, C., van der Plicht, H., Greenwood, A.D., Flemming, C., Agenbroad, L., 2002. Radiocarbon chronologies and extinction dynamics of the late quaternary mammalian megafauna of the taimyr peninsula, Russian Federation. J. Archaeol. Sci. 29, 1017–1042. https://doi.org/10.1006/jasc.2001.0802.

Manley, W.F., 2002. Postglacial Flooding of the Bering Land Bridge: A Geospatial Animation V1. INSTAAR, Univ. Color [WWW Document].

Mann, D.H., Groves, P., Kunz, M.L., Reanier, R.E., Gaglioti, B.V., 2013. Ice-age megafauna in Arctic Alaska: extinction, invasion, survival. Quat. Sci. Rev. 70, 91–108. https://doi.org/10.1016/j.quascirev.2013.03.015.

Markova, A.K., Puzachenko, A.Y., van Kolfschoten, T., van der Plicht, J.,

Ponomarev, D.V., 2013. New data on changes in the European distribution of the mammoth and the woolly rhinoceros during the second half of the Late Pleistocene and the early Holocene. Quat. Int. 292, 4–14. https://doi.org/10.1016/J.QUAINT.2012.11.033.
McCrea, J.M., 1950. On the isotopic chemistry of carbonates and a paleotemperature scale. J. Chem. Phys. 18, 849–857. https://doi.org/10.1063/1.1747785.
Metcalfe, J.Z., Longstaffe, F.J., Jass, C.N., Zazula, G.D., Keddie, G., 2016. Taxonomy, location of origin and health status of proboscideans from Western Canada investigated using stable isotope analysis. J. Quat. Sci. 31, 126–142. https://doi.org/10.1002/jqs.2849.
Metcalfe, J.Z., Longstaffe, F.J., Zazula, G.D., 2010. Nursing, weaning, and tooth development in woolly mammoths from Old Crow, Yukon, Canada: implications for Pleistocene extinctions. Palaeogeogr. Palaeoclimatol. Palaeoecol. 298, 257–270. https://doi.org/10.1016/j.palaeo.2010.09.032.
Mizin, I.A., Sipko, T.P., Davydov, A.V., Gruzdev, A.R., 2018. The wild reindeer (*Rangifer tarandus*: cervidae, Mammalia) on the arctic islands of Russia: a review. Nat. Conserv. Res. 3, 1–14. https://doi.org/10.24189/ncr.2018.040.
Mol, D., Coppens, Y., Tikhonov, A.N., Agenbroad, L.D., MacPhee, R.D.E., Flemming, C., Greenwood, A., Buigues, B., de Marliave, C., van Geel, B., van Reenen, G.B.A., Fisher, D.C., Fox, D., 2001. The Jarkov mammoth: 20,000-year-old carcass of a siberian woolly mammoth Mammuthus primigenius (blumenbach, 1799). In: Proc. 1st Int. Congr. "The World Elephants", pp. 305–309.
Murphy, B.P., Bowman, D.M.J.S., 2006. Kangaroo metabolism does not cause the relationship between bone collagen $\delta^{15}N$ and water availability. Funct. Ecol. 20, 1062–1069. https://doi.org/10.1111/j.1365-2435.2006.01186.x.
Nehlich, O., 2015. The application of sulphur isotope analyses in archaeological research: a review. Earth Sci. Rev. 142, 1–17. https://doi.org/10.1016/J.EARSCIREV.2014.12.002.
Nehlich, O., Richards, M.P., 2009. Establishing collagen quality criteria for sulphur isotope analysis of archaeological bone collagen. Archaeol. Anthropol. Sci. 1, 59–75. https://doi.org/10.1007/s12520-009-0003-6.
Nikolskiy, P., Pitulko, V., 2013. Evidence from the Yana Palaeolithic site, Arctic Siberia, yields clues to the riddle of mammoth hunting. J. Archaeol. Sci. 40, 4189–4197. https://doi.org/10.1016/j.jas.2013.05.020.
Nikolskiy, P.A., Sulerzhitsky, L.D., Pitulko, V.V., 2011. Last straw versus Blitzkrieg overkill: climate-driven changes in the Arctic Siberian mammoth population and the Late Pleistocene extinction problem. Quat. Sci. Rev. 30, 2309–2328. https://doi.org/10.1016/j.quascirev.2010.10.017.
Nogués-Bravo, D., Rodríguez, J., Hortal, J., Batra, P., Araújo, M.B., 2008. Climate change, humans, and the extinction of the woolly mammoth. PLoS Biol. 6, e79. https://doi.org/10.1371/journal.pbio.0060079. https://doi.org/10.1371/journal.pbio.0060079.
O'Connell, T.C., Hedges, R.E.M., 2017. Chicken and egg: testing the carbon isotopic effects of carnivory and herbivory. Archaeometry 59, 302–315. https://doi.org/10.1111/arcm.12253.
Orlova, L.A., Zenin, V.N., Stuart, A.J., Higham, T.F.G., Grootes, P.M., Leshchinsky, S.V., Kuzmin, Y.V., Pavlov, A.F., Maschenko, E.N., 2004. Lugovskoe, Western Siberia: a possible extra-arctic mammoth refugium at the end of the late glacial. Radiocarbon 46, 363–368. https://doi.org/10.1017/S0033822200039667.
Palkopoulou, E., Dalen, L., Lister, A.M., Vartanyan, S., Sablin, M., Sher, A., Nyström Edmark, V., Brandstrom, M.D., Germonpré, M., Barnes, I., Thomas, J.A., 2013. Holarctic genetic structure and range dynamics in the woolly mammoth. Proc. R. Soc. Biol. Sci. 280, 20131910. https://doi.org/10.1098/rspb.2013.1910.
Palkopoulou, E., Mallick, S., Skoglund, P., Enk, J., Rohland, N., Li, H., Omrak, A., Vartanyan, S., Poinar, H., Götherström, A., Reich, D., Dalén, L., 2015. Complete genomes reveal signatures of demographic and genetic declines in the woolly mammoth. Curr. Biol. 25, 1395–1400. https://doi.org/10.1016/j.cub.2015.04.007.
Passey, B.H., Robinson, T.F., Ayliffe, L.K., Cerling, T.E., Sponheimer, M., Dearing, M.D., Roeder, B.L., Ehleringer, J.R., 2005. Carbon isotope fractionation between diet, breath CO_2, and bioapatite in different mammals. J. Archaeol. Sci. 32, 1459–1470. https://doi.org/10.1016/J.JAS.2005.03.015.
Pitulko, V.V., Basilyan, A.E., Pavlova, E.Y., 2014. The berelekh mammoth "graveyard": new chronological and stratigraphical data from the 2009 field season. Geoarchaeology 29, 277–299. https://doi.org/10.1002/gea.21483.
Poinar, H.N., 2006. Metagenomics to paleogenomics: large-scale sequencing of mammoth DNA. Science 311, 392–394. https://doi.org/10.1126/science.1123360.
Potter, B.A., Holmes, C.S., Yesner, D.R., 2013. Technology and economy among the earliest prehistoric foragers in interior eastern Beringia. In: Paleoamerican Odyssey, pp. 81–103.
Putkonen, J., Grenfell, T.C., Rennert, K., Bitz, C., Jacobson, P., Russell, D., 2009. Rain on snow: little understood killer in the north. Eos, Trans. Am. Geophys. Union 90, 221–222. https://doi.org/10.1029/2009EO260002.
Reimer, P.J., Bard, E., Bayliss, A., Beck, J.W., 2013. IntCal13 and Marine13 radiocarbon age calibration curves 0-50,000 years cal BP. Radiocarbon 55, 1869–1887. https://doi.org/10.2458/azu_js_rc.55.16947.
Rees, C.E., Jenkins, W.J., Monster, J., 1978. The sulphur isotopic composition of ocean water sulphate. Geochim. Cosmochim. Acta 42, 377–381.
Rogers, R.L., Slatkin, M., 2017. Excess of genomic defects in a woolly mammoth on Wrangel island. PLoS Genet. 13, e1006601. https://doi.org/10.1371/journal.pgen.1006601.
Saarnisto, M., Karhu, J., 2004. The last mammoths - palaeoenvironment of the Holocene mammoth on Wrangel Island. Quat. Perspect. 14, 126–129.
Schirrmeister, L., Siegert, C., Kuznetsova, T., Kuzmina, S., Andreev, A., Kienast, F., Meyer, H., Bobrov, A., 2002. Palaeoenvironmental and palaeoclimatic records from permafrost deposits in the Arctic region of Northern Siberia. Quat. Int. 89, 97–118. https://doi.org/10.1016/S1040-6182(01)00083-0.
Schmitt, J., Schneider, R., Elsig, J., Leuenberger, D., Lourantou, A., Chappellaz, J., Köhler, P., Joos, F., Stocker, T.F., Leuenberger, M., Fischer, H., 2012. Carbon isotope constraints on the deglacial CO_2 rise from ice cores. Science (80-.) 336, 711–714. https://doi.org/10.1126/science.1217161.
Schwartz-Narbonne, R., Longstaffe, F.J., Metcalfe, J.Z., Zazula, G., Prohaska, T., 2015. Solving the woolly mammoth conundrum: amino acid ^{15}N-enrichment suggests a distinct forage or habitat. Sci. Rep. 5, 9791. https://doi.org/10.1038/srep09791.
Sealy, J., Johnson, M., Richards, M., Nehlich, O., 2014. Comparison of two methods of extracting bone collagen for stable carbon and nitrogen isotope analysis: comparing whole bone demineralization with gelatinization and ultrafiltration. J. Archaeol. Sci. 47, 64–69. https://doi.org/10.1016/j.jas.2014.04.011.
Sealy, J.C., van der Merwe, N.J., Thorp, J.A.L., Lanham, J.L., 1987. Nitrogen isotopic ecology in southern Africa: implications for environmental and dietary tracing. Geochim. Cosmochim. Acta 51, 2707–2717. https://doi.org/10.1016/0016-7037(87)90151-7.
Seuru, S., Leshchinskiy, S., Auguste, P., Fedyaev, N., 2017. Woolly mammoth and man at krasnoyarskaya kurya site, west siberian plain, Russia (excavation results of 2014). Bull. Soc. Géol. Fr. 188, 4. https://doi.org/10.1051/bsgf/2017005.
Sher, A.V., Kuzmina, S.A., Kuznetsova, T.V., Sulerzhitsky, L.D., 2005. New insights into the Weichselian environment and climate of the East Siberian Arctic, derived from fossil insects, plants, and mammals. Quat. Sci. Rev. 24, 533–569. https://doi.org/10.1016/J.QUASCIREV.2004.09.007.
Slobodin, S., 2012. Severochukotsk neolithic culture of the northern far East (genesis, chronology, habitat) [in Russian]. Vestn. SVNTs DVO RAN. Bull. North-East Sci. 2, 110–122.
Sponheimer, M., Robinson, T., Ayliffe, L., Roeder, B., Hammer, J., Passey, B., West, A., Cerling, T., Dearing, D., Ehleringer, J., 2003. Nitrogen isotopes in mammalian herbivores: hair $\delta^{15}N$ values from a controlled feeding study. Int. J. Osteoarchaeol. 13, 80–87. https://doi.org/10.1002/oa.655.
Stuart, A.J., 2015. Late Quaternary megafaunal extinctions on the continents: a short review. Geol. J. 50, 338–363. https://doi.org/10.1002/gj.2633.
Stuart, A.J., 2005. The extinction of woolly mammoth (*Mammuthus primigenius*) and straight-tusked elephant (*Palaeoloxodon antiquus*) in Europe. Quat. Int. 126–128, 171–177. https://doi.org/10.1016/j.quaint.2004.04.021.
Stuiver, M., Reimer, P.J., Reimer, R.W., 2019. CALIB 7.1 [WWW program] [WWW Document].
Stupak, D., 2014. Les assemblages lithiques du site épigravettien de Buzhanka 2 (Ukraine). Anthropologie 118, 538–553. https://doi.org/10.1016/j.anthro.2014.10.012.
Styring, A.K., Fraser, R.A., Arbogast, R.-M., Halstead, P., Isaakidou, V., Pearson, J.A., Schäfer, M., Triantaphyllou, S., Valamoti, S.M., Wallace, M., Bogaard, A., Evershed, R.P., 2015. Refining human palaeodietary reconstruction using amino acid $\delta^{15}N$ values of plants, animals and humans. J. Archaeol. Sci. 53, 504–515. https://doi.org/10.1016/j.jas.2014.11.009.
Surovell, T.A., Grund, B.S., 2012. The Associational critique of quaternary overkill and why it is largely irrelevant to the extinction debate. Am. Antiq. 77, 672–687. https://doi.org/10.7183/0002-7316.77.4.672.
Szpak, P., Gröcke, D.R., Debruyne, R., MacPhee, R.D.E., Guthrie, R.D., Froese, D., Zazula, G.D., Patterson, W.P., Poinar, H.N., 2010. Regional differences in bone collagen $\delta^{13}C$ and $\delta^{15}N$ of Pleistocene mammoths: implications for paleoecology of the mammoth steppe. Palaeogeogr. Palaeoclimatol. Palaeoecol. 286, 88–96. https://doi.org/10.1016/j.palaeo.2009.12.009.
Tejada-Lara, J.V., MacFadden, B.J., Bermudez, L., Rojas, G., Salas-Gismondi, R., Flynn, J.J., 2018. Body mass predicts isotope enrichment in herbivorous mammals. Proc. R. Soc. Biol. Sci. 285, 20181020. https://doi.org/10.1098/rspb.2018.1020.
Tieszen, L.L., Boutton, T.W., Tesdahl, K.G., Slade, N.A., 1983. Fractionation and turnover of stable carbon isotopes in animal tissues: implications for $\delta^{13}C$ analysis of diet. Oecologia 57, 32–37. https://doi.org/10.1007/BF00379558.
Tieszen, L.L., Fagre, T., 1993. Effect of diet quality and composition on the isotopic composition of respiratory CO_2, bone collagen, bioapatite, and soft tissues. In: Prehistoric Human Bone. Springer Berlin Heidelberg, Berlin, Heidelberg, pp. 121–155. https://doi.org/10.1007/978-3-662-02894-0_5.
van Geel, B., Guthrie, R.D., Altmann, J.G., Broekens, P., Bull, I.D., Gill, F.L., Jansen, B., Nieman, A.M., Gravendeel, B., 2011. Mycological evidence of coprophagy from the feces of an Alaskan Late Glacial mammoth. Quat. Sci. Rev. 30, 2289–2303. https://doi.org/10.1016/J.QUASCIREV.2010.03.008.
van Klinken, G.J., 1999. Bone collagen quality indicators for palaeodietary and radiocarbon measurements. J. Archaeol. Sci. 26, 687–695. https://doi.org/10.1006/jasc.1998.0385.
Vartanyan, S.L., 1997. The last Beringian survivors: interdisciplinary palaeogeographical studies on Wrangel Island, East Siberia. In: Beringian Paleoenviron. Work. Progr. Abstr..
Vartanyan, S.L., Arslanov, K.A., Karhu, J.A., Possnert, G., Sulerzhitsky, L.D., 2008. Collection of radiocarbon dates on the mammoths (*Mammuthus primigenius*) and other genera of Wrangel Island, northeast Siberia, Russia. Quat. Res. 70, 51–59. https://doi.org/10.1016/j.yqres.2008.03.005.
Vartanyan, S.L., Garutt, V.E., Sher, A.V., 1993. Holocene dwarf mammoths from Wrangel island in the siberian arctic. Nature 362, 337–340. https://doi.org/10.1038/362337a0.
Veltre, D.W., Yesner, D.R., Crossen, K.J., Graham, R.W., Coltrain, J.B., 2008. Patterns of faunal extinction and paleoclimatic change from mid-Holocene mammoth and polar bear remains, Pribilof Islands, Alaska. Quat. Res. 70, 40–50. https://doi.

org/10.1016/j.yqres.2008.03.006.
Wang, Y., Porter, W., Mathewson, P.D., Miller, P.A., Graham, R.W., Williams, J.W., 2018. Mechanistic modeling of environmental drivers of woolly mammoth carrying capacity declines on St. Paul Island. Ecology 99, 2721–2730. https://doi.org/10.1002/ecy.2524.
Weninger, B., Jöris, O., 2008. A ^{14}C age calibration curve for the last 60 ka: the Greenland-Hulu U/Th timescale and its impact on understanding the Middle to Upper Paleolithic transition in Western Eurasia. J. Hum. Evol. 55, 772–781. https://doi.org/10.1016/J.JHEVOL.2008.08.017.
Weninger, B., Jöris, O., Danzelocke, U., 2007. CalPal-2007. Cologne radiocarbon calibration & paleoclimate research package.
Wißing, C., Matzerath, S., Turner, E., Bocherens, H., 2015. Paleoecological and climatic implications of stable isotope results from late Pleistocene bone collagen, Ziegeleigrube Coenen, Germany. Quat. Res. 84, 96–105. https://doi.org/10.1016/j.yqres.2015.05.005.
Wißing, C., Rougier, H., Crevecoeur, I., Drucker, D.G., Germonpré, M., Krause, J., Naito, Y.I., Posth, C., Schönberg, R., Semal, P., Bocherens, H., 2019. Stable isotopes reveal patterns of diet and mobility in last Neandertals and first modern humans in Europe. Sci. Rep. 9. https://doi.org/10.1038/s41598-019-41033-3.
Wooller, M.J., Zazula, G.D., Edwards, M., Froese, D.G., Boone, R.D., Parker, C., Bennett, B., 2007. Stable carbon isotope compositions of eastern beringian grasses and sedges: investigating their potential as paleoenvironmental indicators. Arctic Antarct. Alpine Res. 39, 318–331.
Zhang, H.-Y., Hartmann, H., Gleixner, G., Thoma, M., Schwab, V.F., 2019. Carbon isotope fractionation including photosynthetic and post-photosynthetic processes in C3 plants: low [CO_2] matters. Geochim. Cosmochim. Acta 245, 1–15. https://doi.org/10.1016/J.GCA.2018.09.035.
Zimov, S.A., Zimov, N.S., Tikhonov, A.N., Chapin, I.S., 2012. Mammoth steppe: a high-productivity phenomenon. Quat. Sci. Rev. 57, 26–45. https://doi.org/10.1016/j.quascirev.2012.10.005.
Zolnikov, I.D., Deev, E.V., Slavinskiy, V.S., Tsybankov, A.A., Rybin, E.P., Lysenko, D.N., Stasyuk, I.V., 2017. Afontova gora II archaeological site: geology and post-depositional deformation (krasnoyarsk, Siberia). Russ. Geol. Geophys. 58, 190–198. https://doi.org/10.1016/j.rgg.2016.04.016.